Corrected Author's Copy. Cite as: Edwards et al. Resolving discrepancies between field and modelled relative sea-level data: lessons from western Ireland. Journal of Quaternary Science 32(7) 957-975. DOI: 10.1002/jqs.2969

Resolving discrepancies between field and modelled relative sea-level data: lessons from western Ireland

Robin Edwards[1*], W. Roland Gehrels[2], Anthony Brooks[1,3], Ralph Fyfe[4], Katie Pullen[4,5], Joseph Kuchar[6], Kieran Craven[1,7]

[1] School of Natural Sciences, Trinity College Dublin, Ireland

[2] Environment Department, University of York, Heslington, YO10 5NG, UK

[3] ABP Marine Environmental Research Ltd, Southampton, UK

[4] School of Geography, Earth and Environmental Sciences, Plymouth University, Plymouth, PL4 8AA, UK

[5] Environment Agency, Horizon House, Deanery Road, Bristol, BS1 5TL, UK

[6] Department of Physics, University of Ottawa, Canada

[7] Department of Geography, Maynooth University, Ireland

[*]Corresponding author: robin.edwards@tcd.ie

Abstract

Accurate reconstruction of late glacial and Holocene relative sea-level (RSL) histories is complicated where mismatches exist between geological data and RSL curves generated by models of glacio-isostatic adjustment (GIA). In Ireland, such discrepancies have profound implications for interpreting the glacial history of the British Isles and for the use of glacial rebound models to predict future sea-level changes. To address this issue we present new RSL data from four sites along the western coast of Ireland, including seventeen data points from the critical time period before 5000 14C a BP for which very few data are available. We generate new RSL simulations from an existing GIA model, incorporating a thickened Irish Ice sheet component. Simulated curves from Co. Mayo and Co. Donegal accommodate the higher than present late glacial RSL inferred from glaciomarine muds whilst still meeting the requirement for below present RSL indicated by the new terrestrial limiting

data points. Relaxation of trimline constraints on maximum ice sheet thickness provides considerable scope for improved GIA performance. These results demonstrate inferences about RSL drawn from GIA modelling and glacio-sedimentary data are not mutually exclusive, and represent a significant step toward resolving a long-standing debate between the field-based and modelling communities.

Keywords: Relative sea-level; Glacial rebound modelling; sea-level index points; British Irish Ice Sheet; late glacial.

Introduction

Concern about the future stability of ice sheets in a warming world has focussed attention on the drivers and mechanisms of ice sheet disintegration (Stocker et al., 2013). Reconstructing the growth and decay of former ice sheets provides important data over centennial to millennial time scales that complement the observational records developed in Greenland and Antarctica. Regional patterns of relative sea-level (RSL) change are strongly controlled by glacio-isostatic adjustment (GIA) which, in turn, is directly related to the varying extent and thickness of an ice sheet over time (Milne, 2015). When used in combination, geologically based RSL reconstructions and numerical models of the GIA process provide powerful constraints on ice sheet and sea-level change in the past, present and future (e.g. Milne et al., 2009; Mitrovica et al., 2015; Peltier et al., 2015).

Sea-level data from the British Isles have played a central role in the iterative process of GIA-model development because the spatially variable and non-monotonic nature of RSL change in the region provides a stringent test of model performance (Lambeck, 1991; Peltier, 1998). This region has particular significance since the demise of the last British-Irish Ice Sheet (BIIS) may serve as a useful analogue for the response of ice sheets with marine-terminating margins (Clark et al., 2012a). The collection of field RSL data combined with GIA modelling complements current efforts to reconstruct the evolution of the BIIS by mapping and dating the deposits it has left behind (Clark, 2014). In addition, these GIA models also play a key role in the prediction of future RSL changes around Britain and Ireland (Lowe et al., 2009; Gehrels, 2010; Shennan et al., 2012).

In Britain, the availability of high quality, widely distributed RSL data has proven especially useful in distinguishing between the influences of earth and ice model components and in tuning associated parameters (e.g. Bradley et al., 2011). However, the paucity of precise RSL data from Ireland places significant constraints on the ability to test and refine the Irish component of the BIIS, with extensive sections of coast lacking any high-quality information (Brooks & Edwards, 2006; Brooks et al., 2008; Edwards & Craven, 2017). Whilst limited data coverage along the eastern coast of Ireland is partially offset by the information available from the adjacent coastline of western Britain, the lacunae along the Irish west coast remain problematic (Figure 1). Addressing these basic knowledge gaps is important given the substantial

discrepancies that exist between the heights of late glacial RSL simulated by GIA modelling and those inferred from elevated glaciomarine sediments (e.g. Lambeck & Purcell, 2001; McCabe et al., 2007; Brooks et al., 2008; Edwards et al., 2008; McCabe, 2008a, 2008b). Although simulated late glacial RSLs typically plot below the heights inferred from glaciomarine sediments along all Irish coasts, the apparent under-prediction is most acute along the western and southern coastlines where discrepancies of several tens of metres are common. Resolving these misfits is particularly significant given current uncertainty surrounding the extent and thickness of grounded ice on the Irish shelf (e.g. Bowen et al., 2002; Greenwood & Clark, 2009; Clark et al., 2012a; Ballantyne & O'Cofaigh, 2017).

This paper begins to redress this deficiency in fundamental RSL data by presenting eleven new sea-level index points (SLIPs) and ten new limiting data points established from four sites along the western coast of Ireland (Figure 1c). The SLIPs provide precise information on the position of past RSL whilst the limiting data indicate whether RSL was above or below a specified level (Shennan, 2015). Seventeen of the twenty-one data points cover the critical time period before 5000 ^{14}C a BP for which very few data are available (Figure 1b). Each of these sites provide pre-Holocene terrestrial limiting dates which constrain the maximum altitude of RSL at the time of deposition and, when combined with existing marine limiting dates from elevated late glacial muds, establish important constraints on possible trajectories of RSL change. These data are used to re-evaluate the apparent discrepancies between field and modelled RSL data and to highlight areas for future development. The results of this study may have implications for other formerly glaciated regions where mismatches occur between field observations and modelled estimates of late glacial to early Holocene RSL change.

Study Area

The region of interest extends from the Fanad Peninsula, Co. Donegal in the north-west of Ireland, to Dingle Bay, Co. Kerry in the south-west (Figure 1c). The four study sites exhibit a range of GIA responses, with higher than present late glacial RSL simulated in Co. Donegal in marked contrast to almost continuously rising RSL from late glacial levels many tens of metres below present in Co. Kerry (Figure 1a). This spatial pattern is consistent with the distribution of qualitative 'raised shoreline'

indicators, although there is an absence of precise RSL data in the form of SLIPs between Dingle and Donegal Bays (Figure 1c).

Notable departures from this general pattern are the higher than present late glacial RSLs at Belderg and Fiddauntawnanoneen in Co. Mayo (Figure 1c), inferred from radiocarbon-dated marine microfossils (McCabe et al., 1986; McCabe et al., 2005; Clark et al., 2012b), and the (undated) elevated deltaic systems at Srahlea and Leenaun in Connemara (Thomas and Chiverell, 2006). Whilst these data cannot precisely fix the former position of RSL, they are interpreted as indicating sea levels several tens of metres above present (McCabe, 2008a,b). The scale of the misfit between these inferences and the model simulations requires a reappraisal of data interpretation and model development (McCabe, 2008b; Edwards et al., 2008). Central to this objective is the need for precise RSL data that permit the former trajectory of RSL change to be more accurately resolved than is possible from the glacio-sedimentary information collected to date. One potential source of such data are sequences of marine and freshwater sediments preserved within elevated rock-bounded basins which have subsequently become isolated from the sea (e.g. Long et al., 2011). Whilst these 'isolation basins' have greatly improved understanding of late glacial RSL change in Scotland (e.g. Shennan et al., 1994, 2000, 2005), similar sites have hitherto proven elusive in Ireland (Thomas and Chiverell, 2006).

Three of the study sites (Ballymichael, Co. Donegal; Rossadilisk, Co. Galway; Lough Fadha, Co. Galway) comprise sediments contained within rock-bounded basins (Figure 2, Figure 3, Figure 4). We use these locations to provide limiting data points which constrain the maximum height of RSL. The fourth study site is located in the inner part of the Shannon estuary where thick intercalated sequences of marine and terrestrial sediments were encountered during site investigations linked to construction of the southern ring road around Limerick (Figure 5). These sediments provide a combination of SLIP and limiting data points, permitting development of a more complete Holocene RSL history at this location. Further details of each study site are available in supplementary information.

Materials and Methods

Field Sampling

Reconnaissance coring was conducted using a combination of open-chamber gouge augering and 'Russian'-type coring. Sediments were logged in the field using the Troels-Smith scheme of stratigraphic notation (Troels-Smith, 1955; Long et al., 1999). Sub-surface sediments were recovered for laboratory analysis using a 'Russian'-type corer (Ballymichael, L. Fhada, Rossadilisk) and a Mostap fixed-piston soil sampler (Shannon estuary). The Mostap corer samples sediments in continuous 2 metre sections, recovering relatively undisturbed material in a porous nylon stocking. Localised sediment disturbance was associated with the cutting shoe which in some instances resulted in small (15-20 cm) gaps in the stratigraphy (see Figure 7). Our dataset also includes 136 engineering boreholes drilled as part of the Limerick Southern Ring Road Phase II (Carter & Barton, 2005). Borehole locations and bedrock heights were surveyed by differential GPS with a vertical precision of ± 10 mm (Shannon, L. Fhada) or by surveying to an established benchmark (Ballymichael, Rossadilisk) with a vertical precision of ± 5 cm. All altitudes are expressed relative to Ordnance Datum Malin (OD), the mean sea level vertical levelling datum for Ireland.

Microfossil Analysis

Selected samples were processed for microfossils (foraminifera, diatoms, pollen). Foraminiferal samples were washed through 500 μm and 63 μm mesh sieves following the methods described by Scott and Medioli (1980). Samples were counted wet under a binocular microscope and identified according to the taxonomy described in Horton and Edwards (2006). Contemporary samples were stained with rose Bengal at the time of collection to distinguish between life and death assemblages. On average, at least 150 tests were identified, and foraminiferal data are expressed as a percentage of the total (dead) foraminiferal tests counted. Diatom samples were processed using standard methods (Battarbee et al., 2001) with a total of 250-300 diatoms identified in each sample to species level where possible following Krammer & Lange-Bertalot (1991a, 1991b, 1997a, 1997b). Ecological (salinity) classifications were made with reference to Denys, (1991-2) and Vos and de Wolf (1993) following Zong & Horton (1998), and diatom counts are expressed as a percentage of the total diatom valves counted. Pollen samples were prepared in accordance with Moore et al. (1991) with the addition of *Lycopodium* tablets to enable calculation of pollen concentration. Pollen taxa were identified using Faegri and Iverson (1964, 1975), Moore and Webb (1978)

and Moore et al. (1991), with minimum counts of >300 total land pollen. Microfossil counts are included as an electronic supplement.

Dating

Samples were submitted for AMS radiocarbon dating to Beta Analytic, USA (Ballymichael, Rossadilisk, Shannon,) and to the NERC Radiocarbon Facility in East Kilbride, UK (L. Fhada) and are reported as conventional radiocarbon years BP with a 1-sigma error (Table S2). Samples were pre-treated with acid/alkali/acid (peat) or acid washes (organic clay), or acid etching (shells). Calendar ages (cal a BP) are calculated using Calib 7.1 (Stuiver et al., 2017) using the IntCal13 calibration dataset for peat/organic clay (Reimer et al., 2013) and expressed with 2-sigma errors (Table S2). Calendar ages derived from shells/foraminifera are processed in a similar manner using the Marine13 calibration dataset (Reimer et al., 2013) with $\Delta R = -33 \pm 48$ years calculated from the 10 nearest points in the marine database (Harkness, 1983; Blake, 2005).

Sea-Level Data and Sample Indicative Meaning

At Ballymichael, Rossadilisk and Lough Fhada, microfossil data are used to determine the presence or absence of marine conditions within the basins. A marine signature indicates that HAT was above the bounding bedrock surface or sill, whilst a freshwater signature evidences HAT below this level. At Ballymichael and Lough Fhada, the exposed bedrock surface and lower sill height are found at +4.8 m OD and +1.35 m OD respectively. At Rossadilisk, the complexity of the bedrock topography precludes definitive identification of minimum surface height over which the basin connects to the open sea. For the purposes of evaluating the evidence for higher than present RSL, we conservatively interpret the absence of marine sediments in the sequence as indicating RSL was lower than present, whilst a marine signature would indicate RSL at or above its current position.

SLIPs in the Shannon estuary are established on the basis of the presence of characteristic assemblages of agglutinated salt-marsh foraminifera (e.g. *Jadammina macrescens, Trochammina inflata, Haplophragmoides* species, and *Miliammina fusca*) found in association with organic-rich sediments. The indicative meaning of each sample is inferred from a foraminiferal transfer function for tide level (Table 1), further details of which are available in supplementary information.

Results

Ballymichael

Two transects comprising ten cores were collected from a grazed, euryhaline marsh currently over four metres above HAT, that is separated from the sea by an elevated bedrock platform and boulder ridge to the north, and a large gravel beach to the west (Figure 2). Coring revealed a topographic hollow in-filled by a sequence of up to four metres of sediment, with the deepest portions of the basin containing grey, clay-rich silts and sands resting on the bedrock surface. In transect A this minerogenic unit is overlain by an organic-rich silty clay above c. +4 m OD which, in turn, grades into a saturated, humified terrestrial peat with abundant wood fragments and plant remains that extends to the modern surface. Transect B traces the contact between clastic and organic sediments down to +3 m OD where the basal silty clay grades conformably into a thin (10 cm) clay-rich peat before being replaced by the humified, woody peat unit.

A core that samples this lowermost transition was collected for microfossil analysis (foraminifera, diatom) and radiocarbon dating to determine environmental context and timing of the onset of organic accumulation. The sequence proved devoid of foraminifera although good concentrations of diatoms were present across the lithostratigraphic transition, permitting counts of c. 250 frustules to be obtained from each sample (Figure 6a). The diatom flora is similar in all samples being strongly dominated by the oligohalobous-indifferent (freshwater) taxa *Flagilaria construens* (20-50% of the sample) with oligohalobous-indifferent taxa typically constituting over 60% of the total population in each sample. Whilst the minerogenic unit lacks any indicator of marine influence, mesohalobous (brackish) taxa account for c. 5% of the population toward the base of the thin clay-rich peat. Low relative abundances of halophobous (salt intolerant) taxa are noted within the humified peat. An AMS radiocarbon date from within the clay-rich peat (+2.86 m OD) returned an age of 11,430 ± 40 ^{14}C a BP.

Rossadilisk

Two transects comprising eight cores were collected from a small salt marsh developed within the protective confines of the bedrock which outcrops across the inter-tidal zone (Figure 3). All cores terminate in contact with a hard surface (likely

bedrock) or coarse sand at between c. -1 and -4 m OD. In the deepest cores a thin unit of silty clay grades upward into a clay-rich peat. Foraminifera are absent from the deepest part of the sequence and diatom analysis across the clay-peat contact reveals that the clay is sterile. However, within the clayey peat and into the overlying more humified, woody peat, high concentrations of oligohalobous-indifferent diatom taxa (c. 80% of the assemblage) are recorded (Figure 6b). Within the woody peat, halophobous species comprise around 15% of the assemblage, indicating accumulation in a freshwater environment. Neither mesohalobous nor polyhalobous diatoms (indicative of saline conditions) are present in any of the samples. An AMS radiocarbon date from the contact between the clay-rich peat and the humified peat returned an age of 12,250 ± 40 ^{14}C a BP. The remainder of the sequence comprises 2 – 5 m of dark peat with wood fragments, which generally becomes increasingly humified with depth. Most cores are capped by a surface veneer of organic sand (c. 10 cm thick) representing the modern salt-marsh surface.

Lough Fhada

Three transects comprising a total of 28 cores were recovered from the tidal marsh at the southwestern end of Lough Fhada. The salt marsh has developed within a small bedrock-bounded basin separated from the sea by two rock sills which are overtopped during high spring tides (Figure 4). Coring terminated against the impenetrable bedrock surface, revealing an irregular, confined basin c. 100 m long by 60 m wide and reaching a maximum depth of almost 12 m.

The sequence commences in a light grey finely laminated clay around 7 cm thick, the laminations taking the form of a tripartite sequence of dark green/black, light grey/white and light brown laminae each c. 1 mm in thickness. The clay is overlain by a well-humified, very dark brown peat which contains very fine sand at the base. This unit becomes slightly less well-humified until it is replaced abruptly by a thin, dark grey clay devoid of organic material. This basal sequence is overlain by a fibrous peat with very fine yellow-brown roots. Where this unit overlies clay, the contact is sharp and fine rootlets are visible penetrating the upper 3 cm of the underlying unit. Towards the margins of the basin beneath c. 0 to -2 m OD, this fibrous peat rests on the underlying bedrock surface. The sequence is capped by up to 4 m of red *Phragmites* peat containing abundant roots and stems, with occasional large pieces of red wood dispersed throughout, which grades progressively from the underlying fibrous peat.

This unit pinches out at the basin margins where the underlying bedrock surface outcrops.

A core from the deepest part of the basin was recovered for microfossil analysis (diatoms, pollen) and radiocarbon dating of the basal sequence (Figure 6c). The diatom flora comprise freshwater taxa, with *Brachysira vitrea* dominating the basal laminated clay and overlying humified peat, with higher relative abundances of *Nitzschia fonticola* associated the laminated clay and in the upper part of the peat into the overlying dark grey clay. A slight increase in brackish taxa is associated with the dark grey clay, but the relative abundance remains low, and polyhalobous species such as *Cocconeis scutellum*, which are present in the uppermost *Phragmites* peat, are absent from the basal sequence.

The pollen data reveal a progressive change from an assemblage dominated by *Rumex acetosa, Empetrum*, *Salix* and *Poaceae* in the laminated clay, through an assemblage comprising *Betula*, *Juniperus, Ericaceae, Cyperaceae* and *Poaceae* in the humified peat and overlying dark grey clay, to an assemblage characterised by *Pinus*, *Corylus*, and *Betula*, with lesser amounts of *Quercus*, *Ulmus,* and *Calluna* (Figure 6c and Supplementary Information). Collectively, this sequence is interpreted as showing the transition from an open environment of scrub and grassland through open woodland to a more closed woodland environment. Radiocarbon dates from the contacts between the laminated clay and the humified peat, the humified peat and the dark grey clay, and the dark grey clay and the yellow rooted peat yielded ages of 11,860 ± 50, 11,150 ± 40 and 10,280 ± 40 ^{14}C a BP, respectively.

Shannon Estuary

A simplified general stratigraphy of the study area based on a dataset of 136 engineering boreholes drilled during construction of the Limerick southern ring road is presented in Figure 5c. Most boreholes terminate in limestone, and this undulating bedrock surface is typically mantled by several metres of glacial diamict, although in some of the topographic hollows, this is replaced by a coarse unit of sand and gravel interpreted as former river channel deposits. The majority of the overlying stratigraphic sequence is dominated by silts and clays, which extend to around +2.5 m OD (comparable to modern high water level). These lengthy minerogenic units contain a number of inter-leaved organic horizons of varying thickness. The organic units are

laterally discontinuous and found across a range of altitudes between c. +1.0 m OD and -17 m OD.

Sediments for laboratory analysis were extracted with a Mostap corer from four locations within the inner Shannon estuary (Figure 7a). The lithostratigraphy in these cores is consistent with the general pattern established by the engineering boreholes and is dominated by fine-grained minerogenic sediments. However, more detailed sediment description reveals a complex sequence of intercalated organic-rich silts, clays, and peat which are summarised below along with accompanying microfossil and radiocarbon data (Figure 7). More detailed, core by core descriptions of the litho-, bio- and chronostratigraphic data are presented in Supplementary Information.

Collectively, the sedimentary sequences from the inner Shannon Estuary record environmental changes spanning the entire Holocene. The earliest portion of the record takes the form of a well-humified freshwater basal peat resting upon diamict which accumulated between 11,100 and 8770 cal a BP within the incised channel of the Shannon River (MS3).

The paired shell-organic radiocarbon dates from the thin lower clay unit which abruptly dissects this peat are clearly out of sequence with respect to the four other dates from within the peat itself (point 17; Figure 7a). The clay is located at the top of a core section and is adjacent to a break in the stratigraphy linked with the coring shoe of the Mostap corer. It is therefore likely that this unit is not *in-situ* but reflects the introduction of younger material brought down from an overlying unit between coring drives. The alternative is that some or all of the peat is detrital in nature, and the stratigraphy reflects deposition of reworked blocks of peat onto estuarine clay. Given the sequential nature of the dates from within the peat, the context of the lower clay unit and its similarity to the material overlying the peat, we regard the former interpretation as the most plausible. On this basis, we establish four terrestrial limiting dates from this basal peat unit (points 12-15; Figure 8). Whilst we consider the lower intercalated clay unit to be reworked, we include it on the age-altitude plot for reference, whilst highlighting its suspect nature (grey symbols).

Sometime after 8770 cal a BP, the coring site at MS3 was inundated resulting in the deposition of around 10 m of silty clay with shells. Inundation followed by rapid accumulation and infilling of accommodation space is recorded in the sediments at

Meelick Creek (MS5). Here, the basal silty sand with shells grades into an estuarine silty clay. The paired foraminifera – bivalve dates produce a pooled mean age of 7700 cal a BP, which is used to establish a marine limiting date (point 16; Figure 8). During this time interval, one or more RSL 'jumps' are inferred from several locations around the world which have been linked to freshwater release during terminal melting of the Laurentide ice sheet (e.g. Hijma & Cohen, 2010; Li et al., 2012; Tornqvist & Hijma, 2012; Lawrence et al., 2016). Whilst our RSL record is not sufficiently detailed to accurately resolve such events, the widespread termination of peat forming communities around -10 m OD (Figure 5c) followed by the creation of sufficient accommodation space to permit rapid sediment accumulation (c. 11 mm/yr), is consistent with an interval of fast RSL rise at this time.

Following this period, a return to more organic sedimentation is recorded in several parts of the inner Shannon (Figure 5c) and is dated in three of the Mostap cores. In MS5, the estuarine silty clays are succeeded by deposition of a 'reed clay' and clayey peat containing salt-marsh foraminifera. The dates from the upper and lower contact of this salt-marsh peat are used to establish two SLIPs (points 3 and 4) which constrain the interval of salt-marsh accumulation to between 6780 – 4420 cal a BP.

During this period, interleaved deposits of organic and minerogenic sediment accumulated in the adjacent sites of Coonagh East (MS4) and Ballinacurra Creek (MS2) reflecting changes in the local balance between RSL and sedimentation. At Coonagh East, the basal organic-rich clay with salt-marsh foraminifera produces a basal SLIP dating to 7340 cal a BP (point 8). This is succeeded by a slowly accumulating (c. 0.9 mm/yr) well-humified peat which is then replaced by a more rapidly accumulating clayey peat containing salt-marsh foraminifera. The radiocarbon dates from the top, middle and bottom of the clayey peat overlap within error and are used to establish 3 SLIPs centred on c. 6500 cal. a BP (points 5-7).

Similar deposits are evident at Ballinacurra Creek, with a humified peat unit slowly accumulating between 7400 to 6300 cal a BP, before being succeeded by a clayey peat which accumulated until c. 5260 cal a BP. The presence of salt-marsh foraminifera in all three of these dated samples permits the establishment of three more SLIPs for this period (points 9-11).

Finally, the clayey peat units of cores MS2, MS4 and MS5 are replaced by grey organic –rich woody clays which in turn give way to heavily iron-stained units that cap the sequences. A further two SLIPs are established from a thin clayey peat unit containing some wood fragments and the remains of salt-marsh foraminifera which dates to between 4140 and 3610 cal a BP (points 1 and 2).

Collectively, the SLIPs and limiting dates reveal a picture of rising RSL during the Holocene within the inner Shannon (Figure 8). The terrestrial and marine limiting dates constrain the possible course of RSL change during the early Holocene. Prior to 9000 cal a BP, RSL was below -15 m OD but had risen above -14 m OD by c. 8000 cal a BP. Inclusion of the (likely) contaminated material from the base of MS3 (grey shaded point 17) does not alter this general picture of change. The long-term rate of RSL decreases after 8000 cal a BP, although scatter in the SLIPS precludes a more detailed assessment of change. The data provide no evidence for higher than present RSL during the Holocene.

Post-depositional lowering of SLIPs by sediment compaction is a potential cause of vertical scatter and has been noted in similar estuarine sequences from Britain (e.g. Shennan & Horton, 2002; Shennan et al., 2002; Edwards et al., 2006; Brain et al., 2011). Whilst only SLIP 8 comes from directly above the pre-Holocene surface and so is regarded as a basal date, SLIPs 5-7 and 11 all come from around a metre or less above the diamict and so are likely to have experienced more limited compaction than those index points overlying thick sedimentary piles. The close agreement between SLIP 4 (MS5) and SLIPs 5-7 (MS4) illustrates the consistency between coring locations and suggests that the influence of compaction on SLIP 4 is also limited.

Modelling of the autocompaction process suggests that post-depositional lowering will be most evident in the middle of organic-rich sequences (Brain et al., 2011; 2012). Consequently, it is likely that SLIPs 1-3 (MS5), and 9-10 (MS2), which are located 2 – 3 metres above the onset of organic accumulation, have all been influenced by this process. On the basis of the offset between SLIP 10 (MS2) and the broadly contemporaneous index points from MS4, it would appear that post-depositional lowering may be of the order of 2 – 3 metres.

Discussion

Significant misfits between simulated RSL curves produced by GIA models and higher than present late glacial RSL positions inferred from glacio-sedimentary data have been noted since the earliest modelling studies in the region (e.g. Lambeck, 1995, 1996). Whilst there has been extensive debate concerning the possible causes of these discrepancies (e.g. McCarroll, 2001; Lambeck & Purcell, 2001; Roberts et al., 2006; McCabe et al., 2007; McCabe, 2008a,b; Edwards et al., 2008), progress has been hampered by the fundamental paucity of high quality RSL data from particular areas and time periods. Here, we briefly evaluate some of these proposed causes with reference to the current generation of GIA models and in light of the new RSL data from W. Ireland.

We employ RSL simulations produced by two recent GIA models developed for Britain and Ireland: the best-fit solution of Bradley et al. (2011), hereafter termed the 'Bradley model'; and the best-fit ('minimal' ice sheet thickness) variant of Kuchar et al. (2012), referred to as the 'Kuchar model'. These models differ slightly from each other (and from earlier modelling iterations) in terms of their upper and lower mantle viscosities, which influence the rate and magnitude of solid earth response to loading and unloading (Table 2). Greater inter-model differences exist in the local ice sheet components that simulate the growth and decay of the BIIS. Whilst the history of the BIIS is imperfectly known, the ice loading term has a significant impact on simulated late glacial RSL and as such, has commonly been cited as a potential cause of poor model performance (e.g. McCabe, 2008b). The inability of GIA models to simulate the high late glacial RSL inferred from field data could be addressed by increasing the ice sheet loading term via some combination of ice sheet thickening, greater spatial extent, earlier advance and later retreat.

GIA ice sheet components are typically based on geological evidence (e.g. moraines, sub-glacial bedforms, erratic carriage, striae etc) and are subject to change as new information becomes available and interpretations are refined. For example, in the early models of Lambeck (1993a, 1993b, 1995), Ireland was not completely ice covered at the LGM and the continental shelf to the south and west was unglaciated. More recent offshore data indicate that a grounded ice sheet extended across much of the continental shelf (Sejrup et al., 2005; Benetti et al., 2010; Dunlop et al., 2010; Clark et al., 2012a; Peters et al., 2015; Ballantyne & Ó Cofaigh, 2017). This spatially extensive ice sheet is represented in the ice sheet component used in the Bradley

model (developed by Brooks et al., 2008). Geological constraints on ice sheet thickness are less abundant than indicators of its extent. Traditionally, the elevation of glacial trimlines has been used to infer the maximum height of the ice sheet surface. In the Bradley model, these are used to calculate ice sheet thickness following correction for the underlying topography, resulting in ice generally less than 500 m thick over the west of Ireland at the LGM (Figure 9). In low-lying regions, such as the Irish midlands, observational constraints on ice sheet thickness are absent and inferences are based on a smoothed overall ice sheet topography. Conversely, if trimlines are re-interpreted as englacial features (Ballantyne et al., 2011; Ballantyne & Ó Cofaigh, 2017), their transformation to indicators of minimum ice sheet height relaxes the vertical constraints used in the Bradley model, opening the way for a thicker ice sheet, greater isostatic depression and higher RSL.

In an alternative to the traditional, geomorphologically-based approach, the Kuchar model uses an ice sheet component developed from the numerical glaciological model of Hubbard et al. (2009). Kuchar et al. (2012) found that the thinnest variant of the suite of models provided by Hubbard et al. (2009) provided the best overall fit with RSL data across Britain and Ireland. This model produces a thicker but much less laterally extensive ice sheet than the Bradley model (Figure 9). The continental shelf and much of south-western Ireland remains unglaciated, whilst maximum loading in the west of Ireland is attained between 21 and 19 ka BP when the simulated ice sheet is up to half a kilometre thick.

In the following sections, we evaluate the relative performance of these contrasting GIA models, examine the field evidence for higher than present late glacial RSL, and discuss potential solutions for any misfits between model simulations and geological reconstructions.

Evaluating the evidence for higher than present RSL in western Ireland

The terrestrial limiting data points from Ballymichael, Rossadilisk and L. Fhada provide new constraints on the maximum height of RSL during the late glacial, and these are plotted alongside existing geological data and simulated RSL generated by the Bradley (solid lines) and Kuchar (dashed lines) models (Figure 10). The terrestrial limiting date from Ballymichael constrains RSL to below ~+2.3 m OD around 13, 300 cal a BP and is consistent with all modelled curves (Figure 10a). This site sits close to

the Holocene zero metre isobase which marks the boundary between coastlines to the east that possess a Holocene RSL high-stand, and those to the west that do not. The east-west gradient is visible in the vertical offsets between the simulated RSL curves of both models (Figure 10a), with higher late glacial RSL predicted in the easternmost location (Corvish) relative to those further west (N. Donegal). The Kuchar model produces the best fit with the existing Holocene SLIPs and terrestrial limiting data which come from west of Ballymichael and indicate the absence of a significant Holocene high-stand (Figure 10b). The Kuchar model predicts substantially higher RSL during deglaciation than the Bradley model, placing RSL at between +70 m OD and +30 m OD during the period covered by the glaciomarine muds at Corvish (Figure 10a). Washing limits at ~+30 m OD are recorded seaward of the Ballycrampsey moraine which was deposited by the ice re-advance that deformed parts of the Corvish sequence (McCabe and Clark, 2003). Notably, whilst even the modest late glacial high-stands of the Bradley model are accompanied by higher than present RSL during the Holocene, the Kuchar model simulates significantly higher deglacial RSL with no Holocene high-stand, reflecting differences in both the ice and earth model components.

The freshwater diatom assemblages and absence of foraminifera in the radiocarbon dated sedimentary sequences at L. Fhada and Rossadilisk (Figure 6b, Figure 6c) constrain the maximum possible height of RSL at these sites during the interval from c. 14,100 cal a BP to c. 12,100 cal a BP (Figure 10c). At L. Fhada, RSL was below -1.4 m OD whilst an upper limit of -2.6 m OD is indicated by the sequence from Rossadilisk. Inferences from both sites are based on the assumption that tidal range has remained unchanged and that the inferred bedrock surface heights are accurate. Modelling work indicates that tidal ranges during the late glacial may have been larger than at present (Uehara et al., 2006; Scourse, 2013) and, if correct, this would serve to lower the maximum inferred position of RSL due to a larger offset between MTL and HAT level. Similarly, since the exposed bedrock heights may only over-estimate the actual minimum elevation of any obscured surfaces, the inferred upper marine limit is a conservative constraint on possible RSL trajectories.

L. Fhada and Rossadilisk are well-positioned to test the hypothesis that a series of subaqueous fans and deltas located around Tullywee and Leenaun, Co. Galway, and Srahlea in Co. Mayo (Figure 1c), may be indicative of regionally high RSL during the

retreat of the Irish Ice Sheet (Thomas & Chiverell, 2006). Whilst acknowledging that the sequences are undated and lacking in marine fauna, Thomas & Chiverell (2006) regarded a glaciolacustrine origin as improbable given the geomorphology and aspect of the sites which face directly onto the open Atlantic Ocean. Instead, they speculated that the sequences may represent 'fjord-head' grounding-line depositional systems that accumulated in association with an elevated RSL of at least +65 m OD.

The four terrestrial limiting data points from L. Fhada and Rossadilisk, plus three existing terrestrial limiting dates from tree stumps and wood peat along the northern shore of Galway Bay, are plotted alongside the modelled RSL curves from the region (Figure 10c). All the radiocarbon-dated terrestrial limiting dates plot above the simulated RSL curves. In contrast, the maximum modelled RSL height in the area during the early phase of deglaciation (-43 m OD at L. Fhada in the Bradley model) is over 100 m below the water level inferred from the elevated deltaic sediments reported by Thomas and Chiverell (2006).

The most compelling support for regionally high late glacial RSL comes from raised glaciomarine muds at Belderg Pier and Fiddauntawnanoneen, along the N. Mayo coastline (Figure 1c). Radiocarbon dating of marine shells and foraminifera found between 0 and +28 m OD, indicates the deposits accumulated between c. 19,000 and 22, 000 cal a BP (McCabe et al., 1986; McCabe et al., 2005). Here we plot the data conservatively as marine limiting dates on the basis that they could have accumulated no higher than HAT, whilst recognising that actual sea levels may have been several metres to tens of metres higher (Figure 10d). In this instance we plot the data alongside the simulated RSL curves for Belderg which differ from those of Rossadilisk and L. Fhada by an average of ~13 m at the time of accumulation. The misfit with the simulated RSL curves is at least 40 m although this rises to over 66 m when considering the data from Fiddauntawnanoneen.

The new data from the inner Shannon indicate that RSL remained at or below present for the duration of the Holocene at this site (Figure 8). These data show generally good agreement with the Bradley model which respects all the limiting dates and plots through the middle of the scattered SLIPs. Interestingly, index points 8 and 11 plot above the curve, indicating the model under-predicts RSL during the interval immediately post-dating the inferred phase of rapid sediment infilling. It was noted that this interval is broadly coeval with the meltwater-induced 'jumps' in sea level reported

519 elsewhere (e.g. Hijma & Cohen, 2010; Li et al., 2012; Tornqvist & Hijma, 2012;
520 Lawrence et al., 2016) which would have created the accommodation space required
521 for rapid sedimentation. The current generation of simulated RSL curves do not
522 include these inferred 'jumps' and so will under-predict RSL during and immediately
523 after such events. In contrast to the Bradley model, the Kuchar model appears to
524 consistently under-predict Holocene RSL, plotting below the basal SLIPs and through
525 the intercalated SLIPs suspected of post-depositional lowering due to compaction.
526 This is consistent with the findings of Kuchar et al. (2012) who note that the greatest
527 misfits are with the Irish field data and overall model performance in this region is
528 poorer than that of Bradley et al. (2011) and Brooks et al. (2008). The more limited
529 lateral extent of the BIIS in the Kuchar model is a likely contributing factor to these
530 misfits (Figure 9).

531 *Implications for existing GIA models*

532 Whilst the Bradley and Kuchar models have reasonably good skill in simulating RSL
533 during the Holocene, their capacity to reliably represent change during the early
534 phases of deglaciation is more equivocal. Despite significant inter-model differences
535 in the BIIS component, both the Bradley and the Kuchar models produce late glacial
536 RSL simulations for the west coast that, whilst similar to each other, plot several tens
537 of metres below the levels inferred from glacio-sedimentary data (Figures 10c and
538 10d). A noteable exception to this general pattern is the relatively good fit of the Kuchar
539 model to the data from Co. Donegal (Figure 10a). This is particularly the case when
540 considering the fact that the Corvish data are plotted conservatively and likely reflect
541 an actual RSL several metres to tens of metres higher.

542 It is particularly significant that, despite simulating a late glacial RSL of over +70 m
543 OD, the Kuchar model does not generate spurious RSL values above present during
544 the Holocene (Figure 10b). The absence of a pronounced Holocene high-stand is
545 noteworthy since the earth model parameters required to achieve a suitable 'best-fit'
546 solution in studies using a thin, trimline-constrained ice sheet, invariably generate
547 higher than present Holocene RSL when late glacial RSL is high (e.g. Brooks et al.,
548 2008; Bradley et al., 2011). In fact, Edwards et al. (2008) suggested that the absence
549 of raised Holocene shorelines along the western coast of Ireland (in marked contrast
550 to their prevalence in the north-east of the country), provided indirect evidence that
551 late glacial RSL was unlikely to have been above present along the Atlantic coast.

Similarly, in their evaluation of RSL along the eastern and southern coasts of Ireland, Lambeck & Purcell (2001) concluded that rising Holocene RSL only a few thousand years after significant late glacial high-stands was incompatible with the fundamental physical responses underpinning the modelling approach.

Relaxation of the trimline constraint provides considerable scope for thickening the BIIS component of current GIA models. In the case of Corvish, the improved fit stems in part from thicker ice cover in the region (~800 m compared to ~300 m in the Bradley model), but also reflects a different response to unloading associated with the selected earth model parameters (Table 2). We briefly explore the potential for a thickened ice sheet to resolve some of the misfits between model simulations and geological reconstructions by re-running the Kuchar et al. (2012) model using the maximal ice model of Hubbard et al. (2009), hereafter termed the 'Kuchar-Max' model. In addition to generating a thicker ice sheet, this model also produces more laterally extensive ice cover and better reflects the inferred timing of ice sheet retreat in the west of Ireland (Figure 9). Under this scenario, western Ireland has continuous ice cover from 25 - 20k cal a BP, with local ice sheet thickness of up to 1 kilometre. We retain the same earth model parameters as employed in the standard Kuchar model in order to illustrate the sensitivity of RSL output to the ice loading term. Further refinement of ice or earth model components, which would require a comprehensive consideration of all RSL data across Britain and Ireland, is beyond the scope of this paper. Instead we use the new and existing RSL data from western Ireland to address the question of whether a thicker ice sheet can produce RSL that simultaneously meets the requirements for high late glacial RSL whilst conforming to the constraints from SLIP and terrestrial limiting data points.

Simulated RSL curves produced by the 'Kuchar-Max' model are plotted alongside the output from the standard 'Kuchar model' for each of the study areas (Figure 11). The simulated RSL curves from Donegal produce late glacial high-stands of between +90 m and +110 m OD whilst plotting below the constraint provided by the terrestrial limiting date from Ballymichael. The Kuchar-Max curve also shows reasonable fit with the Holocene data. Irrespective of whether such extreme late glacial RSLs are accurate, the results demonstrate that these high levels are not physically incompatible with the requirement for a Holocene RSL rising from below present.

At L. Fhada and Rossadilisk, the increased ice loading term elevates the maximum RSL at 20 k cal a BP by over 80 m but, whilst plotting below the terrestrial limiting data points, the RSL still plots significantly (>40 m) below the water levels inferred from the elevated subaqueous fans and deltas in Connemara (Figure 11b). Re-running the Kuchar model with the local (BIIS) loading term removed produces a maximum RSL of around -90 m OD, indicating locally-induced isostatic depression of the order of 155 m is required for the Connemara sequences to be glaciomarine in origin, assuming they date to the most recent phase of deglaciation. Replication of the pattern of change indicated by the RSL curve from Donegal would accommodate these high level deposits whilst conforming to the terrestrial limiting dates from L. Fhada and Rossadilisk. The question thus becomes not one of whether the required RSL response can be simulated, but rather whether the associated requirement for such a thick ice sheet in this area is plausible.

Lastly, RSL simulated by the Kuchar-max model for Belderg Pier is now consistent with the lower / younger marine limiting dates from the glaciomarine muds, although the higher data point from Fiddauntawnanoneen still plots above the RSL curve (Figure 11c). Due to the spatial pattern of isostatic rebound, the simulated curves from the Inner Shannon are similar to those of Belderg Pier, particularly by the onset of the Holocene, and on this basis we plot the two datasets together for illustrative purposes. Simulated maximum RSL generated by the Kuchar-Max model is higher for the inner Shannon, reflecting its more easterly location and thicker ice cover. Interestingly, the Shannon curve can accommodate all the late glacial marine limiting dates from N. Mayo whilst also giving an excellent fit with the Holocene data from the Shannon (Figure 11d). Increasing the extent of grounded ice on the shelf would produce a similar curve for Belderg, suggesting it is possible to reconcile model simulations with the inferences drawn from the elevated marine muds in this area.

The use of trimlines to constrain ice sheet thickness is not unique to Ireland or the Irish component of the BIIS and although their reinterpretation as englacial features may not be universally applicable, a re-assessment of traditional views on ice sheet extent and thickness is required (McCarroll, 2016). For example, Lloyd et al. (2013) note that thicker Scottish ice could potentially resolve the apparent misfits between field and modelled late glacial RSL data from Cumbria, NE England. Our results demonstrate how relaxation of trimline constraints may reconcile apparently divergent late glacial

RSL histories in formerly glaciated regions without negatively impacting model performance during the Holocene.

Summary and Conclusions

New SLIP and limiting data points from three locations in the west of Ireland indicate that RSL has been below present in this region for the past 14,000 years. Additional data from the north-west of Ireland can accommodate RSL slightly above present during this interval, but suggests it was no more than a couple metres higher than its modern level. These new data can be used in combination with existing radiocarbon-dated marine indicators from late glacial glaciomarine muds to constrain trajectories of RSL change since the LGM. Simulated RSL curves produced by recent GIA models are consistent with all of the new data points and show a good fit with the more precise, Holocene SLIPs from the inner Shannon estuary. In contrast, they show less skill in simulating high RSL during the late glacial in Co. Donegal, and underestimate RSL inferred from glaciomarine muds in Co. Mayo by more than 40 m.

New analysis using the thicker ice variant of the GIA model presented by Kuchar et al. (2012) is capable of fitting the late glacial marine limiting dates from both the west and north-west of Ireland, whilst still showing good agreement with the younger terrestrial limiting data points and SLIPs. The simulated curves from Co. Galway do not directly support the hypothesis that nearby subaqueous fans and deltas are glaciomarine in origin (Thomas & Chiverell, 2006). However, the more responsive earth component of the Kuchar-Max model (compared to the Bradley model) is capable of simulating the required RSL high-stand whilst still meeting the requirement for below present RSL indicated by the new terrestrial limiting data points. Whilst thickening of the model ice sheet component has a significant impact on late glacial RSL, its effects on Holocene RSL histories are considerably more muted.

Collectively, our data suggest that the laterally extensive ice sheet employed by Brooks et al. (2008) and Bradley et al. (2011) is too thin over western Ireland, whilst the thicker variants utilised by Kuchar et al. (2012) are too spatially restricted. In a recent review, Knight (2017) noted that the polarisation of views concerning late glacial RSL in Ireland had tended to constrain a more integrated approach to the study of Ireland's deglaciation. We hope the results presented here go some way to addressing this criticism, by demonstrating that inferences drawn from GIA modelling and glacio-

649 sedimentary data are not mutually exclusive. More RSL data, particularly from the late
650 glacial period, are now required to complement ongoing efforts to refine the geometry
651 and dynamics of the BIIS (e.g. Clark, 2014). Relaxation of the trimline constraint on
652 maximum ice sheet thickness provides considerable scope for revising current GIA
653 simulations, not only for Britain and Ireland, but also in other formerly glaciated regions
654 with local ice sheet histories based on similar field evidence.

655 **Acknowledgements**

656 This work was supported by Enterprise Ireland (Grant Number: SC-2003-0215-Y) and
657 the NERC Radiocarbon Facility NRCF010001 (allocation number 1462.0410). We
658 thank the National Roads Authority for funding a number of the radiocarbon dates
659 presented in this paper and for providing access to their archive core data. We also
660 thank Caroline Hillier for assistance with diatom analysis, and Stephen Carter of
661 Headland Archaeology for collaboration on this project. This paper is a contribution to
662 IGCP project 639 'Sea-level change from minutes to millennia'.

References

Ballantyne, C.K., O Cofaigh, C., 2017. The Last Irish Ice Sheet: Extent and Chronology, in: Coxon, P., McCarron, S., Mitchell, F. (Eds.), Advances in Irish Quaternary Studies. Atlantis Press, Paris, France, pp. 101–149. doi:10.29991/978-94-6239-219-9_5

Ballantyne, C.K., McCarroll, D., Stone, J.O., 2011. Periglacial trimlines and the extent of the Kerry-Cork Ice Cap, SW Ireland. Quat. Sci. Rev. 30, 3834–3845.

Bassett, S.E., Milne, G.A., Mitrovica, J.X., Clark, P.U., 2005. Ice sheet and solid earth influences on far-field sea-level histories. Science 309, 925–928. doi: 10.1126/science.1111575

Battarbee, R.W., Jones, V.J., Flower, R.J., Cameron, N.G., Bennion, H., Carvalho, L. and Juggins, S., 2001. Diatoms. In 'Tracking Environmental Change Using Lake Sediments. Volume 3: Terrestrial, Algal, and Siliceous Indicators'.(Eds JP Smol, HJB Birks, and WM Last.) pp. 155–202.

Benetti, S., Dunlop, P., Cofaigh, O., 2010. Glacial and glacially-related features on the continental margin of northwest Ireland mapped from marine geophysical data. J. Maps 14–29. doi:10.4113/jom.2010.1092

Blake, C.B., 2005. Use of maerl as a biogenic archive. Unpublished PhD thesis. Biological Sciences, Queen's University Belfast.

Bowen, D., Phillips, F., McCabe, A.M., Knutz, P., Sykes, G., 2002. New data for the Last Glacial Maximum in Great Britain and Ireland. Quat. Sci. Rev. 21, 89–101. doi:10.1016/S0277-3791(01)00102-0

Bradley, S.L., Milne, G.A., Zong, Y., et al. 2008. Modelling sea-level data from China and Malay–Thai Peninsula to infer Holocene eustatic sea-level change. American Geophysical Union, Fall Meeting 2008, abstract #GC33A-0763.

Bradley, S.L., Milne, G.A., Shennan, I., Edwards, R., 2011. An improved glacial isostatic adjustment model for the British Isles. J. Quat. Sci. 26. doi:10.1002/jqs.1481

Brain, M.J., Long, A.J., Petley, D.N., Horton, B.P., Allison, R.J., 2011. Compression behaviour of minerogenic low energy intertidal sediments. Sediment. Geol. 233, 28–41. doi:10.1016/j.sedgeo.2010.10.005

693 Brain, M.J., Long, A.J., Woodroffe, S. a., Petley, D.N., Milledge, D.G., Parnell, A.C.,
694 2012. Modelling the effects of sediment compaction on salt marsh reconstructions of
695 recent sea-level rise. Earth Planet. Sci. Lett. 345–348, 180–193.
696 doi:10.1016/j.epsl.2012.06.045

697 Brooks, A., Edwards, R., 2006. The development of a sea-level database for Ireland.
698 Irish J. Earth Sci. 24, 13–27.

699 Brooks, A.J., Bradley, S.L., Edwards, R.J., Milne, G.A., Horton, B., Shennan, I., 2008.
700 Postglacial relative sea-level observations from Ireland and their role in glacial
701 rebound modelling. J. Quat. Sci. 23, 175–192. doi:10.1002/jqs.1119

702 Carter, S., Barton, K., 2005. Limerick Southern Ring Road Phase II. Archaeological
703 testing of the estuarine alluvium. Unpublished report to Limerick City Council.

704 Clark, C., 2014. BRITICE-CHRONO: Constraining rates and style of marine-
705 influenced ice sheet decay to provide a data-rich playground for ice sheet modellers.
706 In EGU General Assembly Conference Abstracts Vol. 16, p. 4266.

707 Clark, C.D., Hughes, A.L.C., Greenwood, S.L., Jordan, C., Sejrup, H.P., 2012a.
708 Pattern and timing of retreat of the last British-Irish Ice Sheet. Quat. Sci. Rev. 44, 112–
709 146. doi:10.1016/j.quascirev.2010.07.019

710 Clark, J., McCabe, A.M., Bowen, D.Q., Clark, P.U., 2012b. Response of the Irish Ice
711 Sheet to abrupt climate change during the last deglaciation. Quat. Sci. Rev. 35, 100–
712 115. doi:10.1016/j.quascirev.2012.01.001

713 Denys, L., 1991–92. A check list of the diatoms in the Holocene deposits of the western
714 Belgian coastal plain with a survey of their apparent ecological requirements.
715 Professional Paper 246, Belgian Geological Survey.

716 Dunlop, P., Shannon, R., McCabe, A.M., Quinn, R., Doyle, E., 2010. Marine
717 geophysical evidence for ice sheet extension and recession on the Malin Shelf: New
718 evidence for the western limits of the British Irish Ice Sheet. Mar. Geol. 276, 86–99.
719 doi:10.1016/j.margeo.2010.07.010

720 Edwards, R., Brooks, A., Shennan, I., Milne, G., Bradley, S., 2008. Reply: Postglacial
721 relative sea-level observations from Ireland and their role in glacial rebound modelling.
722 J. Quat. Sci. 23, 821–825. doi:10.1002/jqs.1162

723 Edwards, R., Craven, K., 2017. Relative Sea-Level Change Around the Irish Coast, in:
724 Advances in Irish Quaternary Studies. Atlantis Press, Paris, pp. 181–215.
725 doi:10.2991/978-94-6239-219-9_7

726 Edwards, R.J., 2006. Mid- to late-Holocene relative sea-level change in southwest
727 Britain and the influence of sediment compaction. The Holocene 16, 575–587.

728 Faegri, K., Iversen, J., 1964. Textbook of Pollen Analysis. Second Edition
729 Munksgaard, Copenhagen. 237 pp.

730 Faegri, K., Iversen, J., 1975. Textbook of Pollen Analysis. Third Edition. Munksgaard,
731 Copenhagen, 295 pp.

732 Gehrels, W.R., 2010. Late Holocene land- and sea-level changes in the British Isles:
733 implications for future sea-level predictions. Quat. Sci. Rev. 29, 1648–1660.
734 doi:10.1016/j.quascirev.2009.09.015

735 Greenwood, S.L., Clark, C.D., 2009. Reconstructing the last Irish Ice Sheet 2: a
736 geomorphologically-driven model of ice sheet growth, retreat and dynamics. Quat. Sci.
737 Rev. 28, 3101–3123. doi:10.1016/j.quascirev.2009.09.014

738 Harkness, D.D., 1983. The extent of the natural 14C deficiency in the coastal
739 environment of the United Kingdom, Journal of the European Study Group on
740 Physical, Chemical and Mathematical Techniques Applied to Archaeology PACT 8
741 (IV.9):351-364.

742 Hijma, M.P., Cohen, K.M., 2010. Timing and magnitude of the sea-level jump preluding
743 the 8200 yr event. Geology 38, 275–278. doi:10.1130/G30439.1

744 Horton, B.P., Edwards, R.J., 2006. Quantifying Holocene Sea-Level Change Using
745 Intertidal Foraminifera: Lessons from the British Isles. Cushman Foundation for
746 Foraminiferal Research. Special Publication 40.

747 Hubbard, A., Bradwell, T., Golledge, N., Hall, A., Patton, H., Sugden, D., Cooper, R.,
748 Stoker, M., 2009. Dynamic cycles, ice streams and their impact on the extent,
749 chronology and deglaciation of the British-Irish ice sheet. Quat. Sci. Rev. 28, 758–776.
750 doi:10.1016/j.quascirev.2008.12.026

751 Knight, J., 2017. Deglaciation of the Northern Irish Sea Basin, in: Advances in Irish
752 Quaternary Studies. Atlantis Press, Paris, pp. 151–180. doi:10.2991/978-94-6239-
753 219-9_6

Krammer, K., Lange-Bertalot, H., 1991a. Bacillariophyceae, 3.Teil, Centrales, Fragilariaceae, Eunotiaceae. In: H. Ettl, J. Gerloff, H. Heynig and D. Mollenhauer (Eds.) Süsswasserflora von Mitteleuropa. Band 2/3. Gustav Fischer Verlag, Stuttgart.

Krammer, K., Lange-Bertalot, H., 1991b. Bacillariophyceae, 4.Teil, Achnantaceae. Kritische Ergänzungen zu Navicula (Lineolate) und Gomphonema. In: H. Ettl, G. Gärtner, J. Gerloff, H. Heynig and D. Mollenhauer (Eds.) Süsswasserflora von Mitteleuropa. Band 2/4. Gustav Fischer Verlag, Stuttgaart.

Krammer, K., Lange-Bertalot, H., 1997a. Bacillariophyceae, 1.Teil, Naviculaceae. In: H. Ettl, J. Gerloff, H. Heynig and D. Mollenhauer (Eds.) Süsswasserflora von Mitteleuropa. Band 2/1. Gustav Fischer, Jena.

Krammer, K., Lange-Bertalot, H., 1997b. Bacillariophyceae, 2.Teil, Bacillariaceae, Epithemiaceae, Surirellaceae. In: H. Ettl, J. Gerloff, H. Heynig and D. Mollenhauer (Eds.) Süsswasserflora von Mitteleuropa. Band 2/2. Gustav Fischer, Jena.

Kuchar, J., Milne, G., Hubbard, A., Patton, H., Bradley, S., Shennan, I., Edwards, R., 2012. Evaluation of a numerical model of the British-Irish ice sheet using relative sea-level data: implications for the interpretation of trimline observations. J. Quat. Sci. 27, 597–605. doi:10.1002/jqs.2552

Lambeck, K., 1991. Glacial rebound and sea-level change in the British Isles. Terra Nov. 3, 379–389. doi:10.1111/j.1365-3121.1991.tb00166.x

Lambeck, K., 1993a. Glacial rebound of the British Isles - I. Preliminary model results. Geophys. J. Int. 115, 941–959. doi:10.1111/j.1365-246X.1993.tb01503.x

Lambeck, K., 1993b. Glacial rebound of the British Isles - II. A high-resolution, high-precision model. Geophys. J. Int. 115, 960–990.

Lambeck, K., 1995. Late Devensian and Holocene shorelines of the British Isles and North Sea from models of glacio-hydro-isostatic rebound. J. Geol. Soc. London. 152, 437–448. doi:10.1144/gsjgs.152.3.0437

Lambeck, K., 1996. Glaciation and sea-level change for Ireland and the Irish Sea since Late Devensian/Midlandian time. J. Geol. Soc. London 153, 853–872.

Lambeck, K., Purcell, A.P., 2001. Sea-level change in the Irish Sea since the Last Glacial Maximum: Constraints from isostatic modelling. J. Quat. Sci. 16, 497–506. doi:10.1002/jqs.638

Lawrence, T., Long, A.J., Gehrels, W.R., Jackson, L.P., Smith, D.E., 2016. Relative sea-level data from southwest Scotland constrain meltwater-driven sea-level jumps prior to the 8.2 kyr BP event. Quat. Sci. Rev. 151, 292–308. doi:10.1016/j.quascirev.2016.06.013

Li, Y.X., Törnqvist, T.E., Nevitt, J.M., Kohl, B., 2012. Synchronizing a sea-level jump, final Lake Agassiz drainage, and abrupt cooling 8200years ago. Earth Planet. Sci. Lett. 315–316, 41–50. doi:10.1016/j.epsl.2011.05.034

Lloyd, J.M., Zong, Y., Fish, P., Innes, J.B., 2013. Holocene and Lateglacial relative sea-level change in north-west England: implications for glacial isostatic adjustment models. J. Quat. Sci. 28, 59-70. doi: 10.1002/jqs.2587

Long, A.J., Innes, J.B., Shennan, I., Tooley, M.J., 1999. Coastal stratigraphy: a case study from Johns River, Washington. In: Jones, A.P., Tucker, M.E., and Hart, J. (eds.) The Description and Analysis of Quaternary Stratigraphic Field Sections. Quaternary Research Association Technical Guide No. 7. Quaternary Research Association, Cambridge.

Long, A.J., Woodroffe, S.A., Roberts, D.H., Dawson, S., 2011. Isolation basins, sea-level changes and the Holocene history of the Greenland Ice Sheet. Quat. Sci. Rev. 30, 3748–3768. doi:10.1016/j.quascirev.2011.10.013

Lowe, J. A., Howard, T. P., Pardaens, A., Tinker, J., Holt, J., Wakelin, S., Milne, G., Leake, J., Wolf, J., Horsburgh, K., Reeder, T., Jenkins, G., Ridley, J., Dye, S., Bradley, S., 2009. UK Climate Projections science report: Marine and coastal projections. Met Office Hadley Centre, Exeter, UK.

McCabe, A.M., 2008a. Glacial Geology and Geomorphology: The Landscapes of Ireland. Dunedin Press, Edinburgh.

McCabe, A.M., 2008b. Comment: Postglacial relative sea-level observations from Ireland and the role in glacial rebound modelling. J. Quat. Sci. 23, 817–820.

McCabe, A.M., Clark, P.U., 2003. Deglacial chronology from County Donegal, Ireland: implications for deglaciation of the British-Irish ice sheet. J. Geol. Soc. London. 160, 847–855. doi:10.1144/0016-764903-009

McCabe, A.M., Clark, P.U., Clark, J., 2005. AMS 14C dating of deglacial events in the Irish Sea Basin and other sectors of the British–Irish ice sheet. Quat. Sci. Rev. 24, 1673–1690. doi:10.1016/j.quascirev.2004.06.019

McCabe, A.M., Cooper, J.A.G., Kelley, J.T., 2007. Relative sea-level changes from NE Ireland during the last glacial termination. J. Geol. Soc. London. 164, 1059–1063. doi:10.1144/0016-76492006-164

McCabe, A.M., Haynes, J., MacMillan, N., 1986. Late-Pleistocene tidewater glaciers and glaciomarine sequences from north County Mayo, Republic of Ireland. J. Quat. Sci. 1, 73–84.

McCarroll, D., 2001. Deglaciation of the Irish Sea Basin: A critique of the glaciomarine hypothesis. J. Quat. Sci. 16, 393–404. doi:10.1002/jqs.626

McCarroll, D., 2016. Trimline Trauma: The Wider Implications of a Paradigm Shift in Recognising and Interpreting Glacial Limits. Scottish Geographical Journal. 132, 130–139, doi: 10.1080/14702541.2016.1157203

Milne, G.A., 2015. Glacial isostatic adjustment. In: Shennan I, Long AJ, Horton BP (eds) Handbook of Sea-Level Research. Wiley, Chichester, pp 421-437

Milne, G.A., Gehrels, W.R., Hughes, C.W., Tamisiea, M.E. 2009. Identifying the causes of sea-level change. Nature Geoscience 2, 471-478. doi:10.1038/ngeo544

Mitrovica, J.X., Hay, C.C., Morrow, E., Kopp, R.E., Dumberry, M., Stanley, S. 2015. Reconciling past changes in Earth's rotation with 20th century global sea-level rise: Resolving Munk's enigma. Science Advances 1:e1500679. doi: 10.1126/sciadv.1500679

Moore, P.D., Webb, J.A., 1978. An illustrated guide to pollen analysis. Hodder & Stoughton, London, UK

Moore, P.D., Webb, J.A., Collinson, M.E., 1991. Pollen Analysis. Blackwell Scientific Publications.

Orme, A.R., 1966. Quaternary Change of Sea-Level in Ireland. Trans. Inst. Br. Geogr. 127–140.

Peltier, W.R., 1998. Postglacial variations in the level of the sea: Implications for climate dynamics and solid-Earth geophysics. Rev. Geophys. 36, 603–689. doi:10.1029/98RG02638

Peltier, W.R., Argus, D.F., Drummond, R. 2015. Space geodesy constrains ice age terminal deglaciation: The global ICE-6G_C (VM5a) model, J. Geophys. Res. Solid Earth, 120, 450–487, doi:10.1002/2014JB011176

Peters, J.L., Benetti, S., Dunlop, P., Ó Cofaigh, C., 2015. Maximum extent and dynamic behaviour of the last British–Irish Ice Sheet west of Ireland. Quat. Sci. Rev. 128, 48–68. doi:10.1016/j.quascirev.2015.09.015

Reimer, P., Bard, E., Bayliss, A., 2013. IntCal13 and Marine13 radiocarbon age calibration curves 0–50,000 years cal BP. Radiocarbon 55, 1869–1887.

Roberts, D., Chiverrell, R., Innes, J., Horton, B., Brooks, A., Thomes, G., Turner, S., Gonzales, S., 2006. Holocene sea levels, Last Glacial Maximum glaciomarine environments and geophysical models in the northern Irish Sea Basin, UK. Mar. Geol. 231, 113–128. doi:10.1016/j.margeo.2006.05.005

Scott, D.B., Medioli, F.S., 1980. Quantitative studies of marsh foraminifera distribution in Nova Scotia: implications for sea-level studies. Journal of Foraminiferal Research, Special Publication 17: 1-58.

Scourse, J., 2013. Quaternary - sea-- level and palaeotidal changes : a review of impacts on, and responses of, the marine biosphere. Oceanogr. Mar. Biol. An Annu. Rev. 51, 1–70.

Sejrup, H.P., Hjelstuen, B.O., Dahlgren, K.I.T., Haflidason, H., Kuijpers, A., Nygård, A., Praeg, D., Stoker, M.S., Vorren, T.O., 2005. Pleistocene glacial history of the NW European continental margin. Mar. Pet. Geol. 22, 1111–1129. doi:10.1016/j.marpetgeo.2004.09.007

Shennan I. 2015. Handbook of sea-level research: framing research questions. In Handbook of Sea- Level Research, Shennan I, Long AJ, Horton BP (eds). Wiley, Chichester; 3-25.

Shennan, I., Hamilton, S., Hillier, C., Woodroffe, S., 2005. A 16000-year record of near-field relative sea-level changes, northwest Scotland, United Kingdom. Quat. Int. 133–134, 95–106. doi:10.1016/j.quaint.2004.10.015

Shennan, I., Horton, B., 2002. Holocene land- and sea-level changes in Great Britain. J. Quat. Sci. 17, 511–526. doi:10.1002/jqs.710

Shennan, I., Innes, J.B., Long, A.J., Zong, Y., 1994. Late Devensian and Holocene relative sea-level changes at Loch nan Eala, near Arisaig, northwest Scotland. J. Quat. Sci. 9, 261–283.

Shennan, I., Lambeck, K., Horton, B., Innes, J., Lloyd, J., McArthur, J., Purcell, T., Rutherford, M., 2000. Late Devensian and Holocene records of relative sea-level changes in northwest Scotland and their implications for glacio-hydro-isostatic modelling. Quat. Sci. Rev. 19, 1103–1135. doi:10.1016/S0277-3791(99)00089-X

Shennan, I., Milne, G., Bradley, S., 2012. Late Holocene vertical land motion and relative sea-level changes: lessons from the British Isles. J. Quat. Sci. 27, 64–70. doi:10.1002/jqs.1532

Stocker, T.F., Qin, D., Plattner, G.K., Tignor, M., Allen, S.K., Boschung, J., Nauels, A., Xia, Y., Bex, B., Midgley, B.M., 2013. IPCC, 2013: climate change 2013: the physical science basis. Contribution of working group I to the fifth assessment report of the intergovernmental panel on climate change.

Stuiver, M., Reimer, P.J., and Reimer, R.W., 2017, CALIB 7.1 [WWW program] at http://calib.org

Thomas, G.S.P., Chiverrell, R.C., 2006. A model of subaqueous sedimentation at the margin of the Late Midlandian Irish Ice Sheet, Connemara, Ireland, and its implications for regionally high isostatic sea-levels. Quat. Sci. Rev. 25, 2868–2893. doi:10.1016/j.quascirev.2006.04.002

Törnqvist, T.E., Hijma, M.P., 2012. Links between early Holocene ice-sheet decay, sea-level rise and abrupt climate change. Nat. Geosci. 5, 601–606. doi:10.1038/ngeo1536

Troels-Smith, J. 1955. Characterisation of unconsolidated sediments. Danmarks Geologiske Undersøgelse IV 3: 1-73.

Uehara, K., Scourse, J.D., Horsburgh, K.J., Lambeck, K., Purcell, A.P., 2006. Tidal evolution of the northwest European shelf seas from the Last Glacial Maximum to the present. J. Geophys. Res. 111, 1–15. doi:10.1029/2006JC003531

903 Vos, PC, de Wolf, H. 1993. Diatoms as a tool for reconstructing sedimentary
904 environments in coastal wetlands; methodological aspects. Hydrobiologia 269/270,
905 285-296.

906 Zong, Y., Horton, B.P., 1998. Diatom zones across intertidal flats and coastal
907 saltmarshes in Britain. Diatom Res. 13, 375–394
908 doi:10.1080/0269249X.1998.9705456

909

List of Figures

Figure 1: (A) Simulated RSL curves produced by three glacial rebound models (Brooks et al., 2008; Bradley et al., 2011; Kuchar et al., 2012) illustrating the contrasting patterns of RSL change predicted along the western coast of Ireland. (B) Age distribution (radiocarbon years BP) of sea-level data points for the west of Ireland classified according to the categories in the Irish sea-level database (Brooks & Edwards, 2006) 'Primary' SLIPs possess accurate information on location, altitude, age, and indicative meaning with associated error terms. For 'Secondary' SLIPs, one or more of the core variables is unquantified or associated with significant uncertainty. 'Primary' limiting dates are considered to be *in situ* and, whilst lacking an indicative meaning, come from contexts in which the age and depositional environment is clear. For 'Secondary' limiting dates, one or more of these criteria is not met (e.g. the nature of the depositional environment is contested, or material is potentially reworked). (C) Spatial distribution of sea-level data points along the western coast of Ireland illustrating the paucity of precise RSL data (red squares) along much of the coast. Colour coded categories as in B. Location of study sites indicated by red stars. Distribution of raised shorelines and location of the zero metre isobase adapted from Orme (1966).

FIGURE 2: (A) Location and (B) site maps of the study site at Ballymichael, Co. Donegal. (C) Summary lithostratigraphy of both transects indicating sample core and radiocarbon date.

FIGURE 3: (A) Location and (B) site maps of the study site at Rossadilisk, Co. Mayo. Legend as in Figure 2B. Dark blue shading indicates inter-tidal areas. (C) Summary lithostratigraphy of both transects indicating sample core and radiocarbon date.

FIGURE 4: (A) Location and (B) site maps of the study site at Lough Fhada, Co. Mayo. Legend as in Figure 2. (C) Summary lithostratigraphy of all transects indicating sample core.

FIGURE 5: (A) Location and (B) site maps of the study area in the Shannon estuary. Dark blue shading indicates inter-tidal areas. Surface foraminiferal sampling locations (A inset) shown as red squares (1 = Carrigaholt; 2 = Querrin; 3 = Blackweir Bridge; 4 = Moyasta; 5 = Carrig Island; 6 = Knock; 7 = Aughinish; 8 = Islandavanna; 9 =

Ringmoylan). (C) Summary lithostratigraphy derived from engineering borehole data (black circles). Mostap core locations shown as red circles.

FIGURE 6: Summary diatom data for (A) Ballymichael, (B) Rossadilisk and (C) Lough Fhada, with additional pollen data for L. Fhada. Lithostratigraphy as in Figures 2-4. Black squares indicate positions of microfossil samples. Red squares indicate radiocarbon dates.

FIGURE 7: Litho-, bio- and chrono-stratigraphy from the Mostap cores recovered from the inner Shannon estuary. (A) Lithostratigraphy of sample cores indicating the position of material sampled for radiocarbon dating. Red squares indicate samples used to establish sea-level index points, whilst green and blue triangles indicate terrestrial and marine dates respectively (see text for details). Summary foraminiferal diagrams indicate assemblages associated with the radiocarbon dated samples in cores MS5 (B), MS4 (C), MS3 (D) and MS2 (E).

FIGURE 8: Sea-level index points and limiting dates from the Shannon estuary plotted alongside the modelled RSL curves of Bradley et al. (2011) and Kuchar et al. (2012). Grey triangles indicate out of sequence dates (see text for details).

FIGURE 9: Ice sheet thickness in metres at 24, 21, 19 and 16 k cal. a BP for the three GIA models. Minimal = minimal ice sheet thickness variant of Kuchar et al. (2012) – 'Kuchar model'; Maximal = maximal ice sheet thickness variant of Kuchar et al. (2012) – 'Kuchar-Max model'; Bradley = ice sheet component used in Bradley et al. (2011) – 'Bradley model'.

FIGURE 10: Sea-level index points and limiting dates plotted alongside modelled RSL curves for: Corvish, Ballymichael and N. Donegal (A, B); L. Fhada and Rossadilisk (C); the Inner Shannon and Belderg Pier (D). Symbols as in Figure 8.

FIGURE 11: Sea-level index points and limiting dates plotted alongside modelled RSL curves for: Corvish, and Ballymichael (A); L. Fhada and Rossadilisk (B); the Inner Shannon and Belderg Pier (C); and the Holocene portion of the Inner Shannon (D). Symbols as in Figure 8.

		Calibrated Age (Cal. a BP)		Sample Altitude (m OD)		Tidal Elevation (m relative to MTL)		Palaeo Mean Tide Level (m OD)		
Site	Manuscript Code	Min	Max	Altitude	Error	Elevation	Error	PMTL	Error	Date Type
Ballymichael	-	13155	13375	4.8	0.5	2.48	0.30	2.32	0.58	Upper Lim
Rossadilisk	-	14004	14237	0	0.5	2.59	0.30	-2.59	0.58	Upper Lim
L Fhada	-	11828	12375	1.35	0.1	2.71	0.30	-1.36	0.32	Upper Lim
L Fhada	-	12876	13106	1.35	0.1	2.71	0.30	-1.36	0.32	Upper Lim
L Fhada	-	13567	13766	1.35	0.1	2.71	0.30	-1.36	0.32	Upper Lim
Meelick (MS5)	1	3618	3880	0.85	0.1	2.96	0.50	-2.11	0.51	SLIP
Meelick (MS5)	2	3874	4138	0.66	0.1	3.04	0.50	-2.38	0.51	SLIP
Meelick (MS5)	3	4417	4783	-0.54	0.1	2.96	0.50	-3.50	0.51	SLIP
Meelick (MS5)	4	6562	6778	-1.33	0.1	2.97	0.50	-4.30	0.51	SLIP
Coonagh East (MS4)	5	6485	6711	-1.03	0.1	2.88	0.50	-3.91	0.51	SLIP
Coonagh East (MS4)	6	6311	6562	-1.25	0.1	2.97	0.50	-4.22	0.51	SLIP
Coonagh East (MS4)	7	6322	6558	-1.44	0.1	2.93	0.50	-4.37	0.51	SLIP
Coonagh East (MS4)	8	7256	7424	-2.15	0.1	2.93	0.50	-5.08	0.51	SLIP
Ballinacurra (MS2)	9	5057	5459	-1.8	0.1	2.89	0.50	-4.69	0.51	SLIP
Ballinacurra (MS2)	10	6215	6412	-2.87	0.1	3.05	0.50	-5.92	0.51	SLIP
Ballinacurra (MS2)	11	7306	7551	-3.67	0.1	3.00	0.50	-6.67	0.51	SLIP

Coonagh Pt. (MS3)	12	8770	9128	-11.76	0.1	3.25	1.00	-15.01	1.00	Upper Lim
Coonagh Pt. (MS3)	13	10237	10482	-12.44	0.1	3.25	1.00	-15.69	1.00	Upper Lim
Coonagh Pt. (MS3)	14	10298	10741	-12.6	0.1	3.25	1.00	-15.85	1.00	Upper Lim
Coonagh Pt. (MS3)	15	10741	11121	-13	0.1	3.25	1.00	-16.25	1.00	Upper Lim
Meelick (MS5)	16	7493	7770	-11.71	0.1	1.38	1.00	-13.09	1.00	Lower Lim
Meelick (MS5)	16	7682	8049	-11.71	0.1	1.38	1.00	-13.09	1.00	Lower Lim
Coonagh Pt. (MS3)	17	8454	8645	-12.87	0.1	1.38	1.00	-14.25	1.00	Lower Lim
Coonagh Pt. (MS3)	17	7973	8269	-12.87	0.1	1.38	1.00	-14.25	1.00	Lower Lim

Table 1: Relative sea-level data. Tidal elevation is the height relative to mean tide level at which the sea-level indicator formed (also termed the 'indicative meaning'). SLIP = sea-level index point derived from the foraminiferal transfer function; Upper Lim. = Terrestrial limiting data point; Lower Lim. = Marine limiting data point.

Model Parameter	Brooks model	Bradley model	Kuchar model	Kuchar-Max model
Lithospheric thickness (km)	71	71	71	71
Upper mantle viscosity (Pa S)	4×10^{20}	$4 – 6 \times 10^{20}$	3×10^{20}	3×10^{20}
Lower mantle viscosity (Pa S)	4×10^{22}	$3 – 6 \times 10^{22}$	2×10^{22}	0.8×10^{22}
Local ice sheet component (British Irish Ice Sheet)	Derived from field data Trimline constrained Thin but laterally extensive	Same as the Brooks model	Derived from thermomechanical numerical ice sheet model (Hubbard et al., 2009) – minimal Thicker but less laterally extensive than Brooks model	Derived from thermomechanical numerical ice sheet model (Hubbard et al., 2009) – maximal Thicker than Kuchar model. Intermediate in lateral extent between Brooks and Kuchar models
Non-local ice model ('eustatic' term)	Bassett et al. (2005) Slow-down at 6 ka. Post-modelling correction (~5 m rise between 7 – 2 ka)	Bradley et al. (2008) Initial slow-down at 7 ka. Melting ends by 1 ka.	Same as Bradley model	Same as Bradley model

Table 2: Summary of published GIA model parameters for: the 'Brooks model' (best-fit solution of Brooks et al., 2008); the 'Bradley model' (best-fit solution of Bradley et al., 2011); the 'Kuchar model' (minimal ice thickness variant of Kuchar et al., 2012); the 'Kuchar-Max model' (maximal ice thickness variant of Kuchar et al., 2012). The Kuchar-Max model simulations used in this paper employ the same earth model parameters as the Kuchar model (see text for details) but are driven by the local ice sheet of the maximal simulation.

Resolving discrepancies between field and modelled relative sea-level data: lessons from western Ireland– Supplementary Information

Site Descriptions

Ballymichael, Co. Donegal

Ballymichael is a small hamlet situated on the north coast of the Fanad peninsula in Co. Donegal (Figure 1c, 2a). The irregular, rocky coastline of the peninsula comprises resistant headlands of Precambrian bedrock flanked by beaches of gravel or sand, which are often associated with dune systems. The study site is a grazed euryhaline marsh forming within a semi-enclosed basin, separated from the Malin Sea by an elevated bedrock platform and boulder ridge to the north, and a large gravel beach to the west (Figure 2b).The area is mesotidal (Table S1) and characterised by high wave energy dominated by Atlantic swells, with a 50 year extreme wave height of 30 m (Orford, 1989; Carter, 1990). The study site is currently over four metres above highest astronomical tide (HAT) and is afforded some protection from the largest waves by the exposed rock promontories of Sloddan and Easkin to the west. At its seaward margin, the rock surface descends beneath the gravel beach but a small (<1 m) drainage ditch exposes buried bedrock at +4.8 m OD. On this basis, we interpret the presence of freshwater sediment within the basin as indicative of a marine limit no higher than +4.8 m OD at the time of deposition.

The Fanad peninsula was ice-covered during the last glacial maximum (LGM), with ice radiating from the Donegal Ice Dome and extending offshore. Radiocarbon dating of foraminifera within glaciomarine muds at Corvish in Trawbreaga Bay (Figure 1c) indicates that the area to the east of the study site was ice-free by 21k cal a BP, although a subsequent short-lived re-advance into the bay (the Ballycramspey re-advance) is inferred between c. 17 – 18k cal a BP (McCabe & Clark, 2003). ^{10}Be exposure dates from the Errigal-Muckish mountains imply residual ice cover may have persisted at higher elevations until ~16k cal a BP (Ballantyne et al., 2013; Ballantyne & O'Cofaigh, 2017).

The radiocarbon-dated glaciomarine muds at Corvish indicate higher than present late glacial RSL and are consistent with qualitative raised shoreline indicators between approximately +20 to +30 m OD. Stephens & Synge (1965) identify three possible late glacial shorelines in the region, each possessing a different gradient but all dipping

westward. A similar suite of postglacial shoreline features below ~+5 m OD is interpreted as indicating a Holocene high-stand, with a westward limit represented by the zero metre isobase of Orme (1966), beyond which raised shorelines are largely absent (Figure 1c). The Irish RSL database contains three SLIPS from N. Donegal and a further eight terrestrial limiting dates in addition to the data from Corvish (Brooks & Edwards, 2006). The SLIP data which come from salt-marsh peat at Clonmass and Ballyness (Shaw, 1985; Shaw & Carter, 1994), place RSL below present since the mid-Holocene, whilst the terrestrial limiting dates from freshwater peat and wood constrain RSL to below ~+3 m OD.

Rossadilisk, Co. Galway

The site at Rossadilisk, Co. Galway is located on the margins of the entrance to Lough Atalia, adjacent to Cleggan Bay (Figure 3a, 3b). Here, patchy salt marsh has developed within the protective confines of the Siluro-Devonian granite bedrock which outcrops extensively within the inter-tidal zone. The area is macrotidal (Table S1) and experiences high wave energy (Orford, 1989; Carter, 1990; Devoy, 1992). Whilst the study site is sheltered from waves by a series of small islands and the Aughrus peninsula, a thin veneer of sand over much of the salt-marsh surface suggests it still experiences intervals of higher energy deposition.

During the late glacial, the site was ice covered with ice moving in a general east-west direction (e.g. Finch, 1977). The glacial stratigraphy of the region has limited chronological control, although a suite of ^{10}Be exposure ages from Connemara and around the margins of Clew Bay indicate ice free conditions no later than ~15k a BP (Ballantyne & O'Cofaigh, 2017). Much of the land in the immediate vicinity of the site is characterised by exposed bedrock, sometimes with a thin topsoil cover although till and drumlins are present nearby. The complexity of the buried bedrock surface prevents unambiguous identification of a single sill connecting the basin with the open sea. For the purposes of evaluating the evidence for higher than present RSL, we conservatively interpret the presence of marine sediments within the basin as indicating RSL was at least as high as today, whilst the absence of marine sediments suggests RSL was lower than present.

No precise RSL data are available from this area but an extensive suite of terrestrial limiting dates from freshwater peat at Carrownisky and Silver Strand, south of Clew

Bay, demonstrate that RSL has been below present for the last 5000 years (Delaney & Devoy, 1995; Devoy et al., 1996; Williams & Doyle, 2014).

Lough Fhada, Co. Galway

Lough Fhada is a small bedrock-bounded basin separated from the sea by two rock sills at 1.86 m OD and 1.35 m OD (Figure 4). Its underlying geology and glacial history is similar to that of Rossadilisk which lies less than 50 km to the north-west. At present, the sea overtops these sills during high spring tides and the basin is filled with brackish water which supports salt-marsh vegetation. During times of lower RSL, the rock sills will exclude marine water resulting in the deposition of freshwater deposits in an 'isolation' basin. On this basis, we interpret the presence of freshwater sediments as indicative of a marine limit no higher than +1.35 m OD.

No precise RSL data are available from this area although terrestrial limiting dates based on freshwater peat and wood have been reported from around Galway Bay where extensive exposures of wood peat have been sampled between Spiddal and Galway City, limiting RSL to below present since c. 7.5k cal a BP (Williams & Doyle, 2014).

Inner Shannon

The final study area is located in the Inner Shannon estuary, west of Limerick city, and encompasses predominantly reclaimed land flanking the river, extending between Meelick and Ballinacurra Creeks (Figure 5a, 5b). The estuary is macrotidal (Table S1) and tidal waters account for 70% of the volume of the upper estuary (Wheeler and Healy, 2001). Extensive inter-tidal flats are exposed at low water, whilst the adjacent land is low-lying and fringed by marsh and reed bed habitats (Curtis and Sheehy-Skeffington, 1998). These environments were more extensive in the past, but several centuries of embanking and draining has reclaimed at least 6 500 ha (Healy & Hickey, 2002; Hickey & Healy, 2005). The resulting narrowing of the estuary and loss of inter-tidal area may have increased the tidal range, although the extent of any change is unknown. As reconstructed tidal elevations are calculated using modern tidal data, the impact of any amplification will be a tendency to under-estimate former RSL position prior to reclamation.

The underlying geology is Carboniferous in age and the study area in the inner estuary rests on limestone and shale. The region was ice covered during the Late Midlandian

glaciation (MIS 2) and, whilst the precise sequence and chronology of ice-sheet advance and retreat is poorly constrained, the estuary was likely ice free at or shortly after 19k cal a BP (Ballantyne & O'Cofaigh, 2017).

Precise sea-level data within the Shannon estuary are lacking (Wheeler and Healy, 2001), and the limits of RSL during the mid to late Holocene can only be tentatively inferred from inter-tidal archaeology (see O'Sullivan, 2001). Radiocarbon-dated wood from posts or tree trunks suggests RSL was at least five metres below present c. 6500 cal a BP (O'Sullivan, 2001). In the outer estuary at Rinevella Bay, wood and freshwater peat exposed in the inter-tidal zone constrain RSL to below present c. 4800-3600 cal a BP (Pearson, 1979). Due to its length and orientation, GIA models produce different simulated RSL curves for locations in the inner and outer estuary (Lambeck, 1996; Brooks et al., 2008) suggesting comparison of data from sites throughout the system can only be meaningfully attempted following correction for this differential effect. Consequently, we do not present data from outer Shannon locations when plotting our results from the inner Shannon site.

Foraminiferal Transfer Function

Extensive drainage and land reclamation has significantly altered the coastal environments within the Shannon estuary. This precludes the collection of a sufficiently large dataset of reliable modern analogue assemblages to permit the development of a local foraminiferal transfer function. Consequently we employ the weighted averaging partial least squares (WA-PLS) transfer function compiled from the large surface dataset (200 samples) of Horton & Edwards (2006). This combines data from 15 sites in Britain and Ireland and includes two transects from the west coast of Ireland. Calculations are made using the C2 program (ver. 1.7.7, Juggins, 2014) following normalisation of height data to account for inter-site variations in tidal range (see Horton & Edwards, 2006). We calculate dissimilarity using the modern analogue technique (MAT) and consider fossil samples with coefficients below the tenth percentile as having good analogues in the training set.

We first tested the applicability of this transfer function by using it to predict the elevation of 29 surface samples collected from nine locations within the Shannon estuary (Figure 5a). Figure S1 shows the foraminifera-predicted elevation plotted with the observed elevation following normalisation of all height data. The transfer function

predicts within error the observed sample elevations of 23 of the 29 samples. Of the six erroneous estimates, three come from samples with poor or no analogues in the training set which would be excluded from any reconstruction. Similarly, a further two samples are recovered from low elevation, organic-poor sediments at or below mean high water of neap tides (MHWNT) which are not environments sampled for RSL reconstruction in our study due to the potential for reworking.

On the basis of these data, we analyse the foraminiferal content of organic sediments sent for radiocarbon dating and establish SLIPs utilising transfer function reconstructions when the fossil assemblages have a good modern analogue in the training set (see Table 1). Where foraminifera are absent or assemblages do not possess a good modern analogue, the indicative meaning of the dated sample cannot be reliably established and it is treated as a limiting data point. Terrestrial limiting dates are considered to indicate deposition at or above HAT. Marine limiting dates are considered to indicate deposition below MHWNT and are established where foraminiferal samples from minerogenic sediments contain typical estuarine assemblages dominated by calcareous taxa.

Inner Shannon Mostap Core Litho-, Bio- and Chronostratigraphic Descriptions.

At Meelick Creek (MS5) just over 16.5 m of sediment were recovered from within a channel incised in bedrock, underlying the modern Crompaun River (Figure 5b, Figure 7a). The sequence terminates in stiff, over-consolidated clay, equivalent to the diamict unit described in the engineering boreholes. This pre-Holocene surface is unconformably overlain by c. 2 m of silty sand with small shells, which grades into finer grained grey silty clay with occasional shells above 1345 cm depth. Foraminifera are abundant within the silty clay with the assemblage dominated by *Ammonia* species and a range of other calcareous taxa typical of deposition in an estuarine environment (Figure 7b). The presence of small numbers of the agglutinated salt-marsh foraminifera *T. inflata* supports this estuarine interpretation, indicating the existence of vegetated inter-tidal environments in the vicinity. An AMS radiocarbon date from a monospecific sample of *Ammonia* at 1331 cm depth returned an age of 7390 ± 70 ^{14}C a BP. A small bivalve shell (unidentified species) from the same sample was similarly dated to 7120 ± 50 ^{14}C a BP.

The early Holocene estuarine silty clay is succeeded by a dark grey organic-rich clay containing the stems and leaves of *Phragmites*. This 'reed clay' extends from 420 – 300 cm depth where it grades progressively into a more humified clayey peat. A foraminiferal sample from just above this transition contains a very low abundance assemblage dominated by *J. macrescens* (>80%) with a few *M. fusca* and *T. inflata*, which is characteristic of a salt-marsh environment (Horton & Edwards, 2006). An AMS radiocarbon date from this peat indicates that reed swamp environments had given way to salt-marsh by 5860 ± 40 ^{14}C a BP.

The thin, salt-marsh peat grades progressively into a very organic clay with indeterminate woody fragments (stems / roots). Foraminiferal analysis over this contact shows a similar salt-marsh assemblage to that of the peat unit (Figure 7b), but with the presence of small numbers of *Haplophragmoides* which are typically associated with low salinity conditions (de Rijk, 1995). The AMS radiocarbon age of 4030 ± 40 ^{14}C a BP from this contact dates a shift to more minerogenic sedimentation which extends from 214 – 100 cm depth. The organic content of this clay-rich unit increases up core, with detrital wood, reed stems and small shells dispersed throughout, culminating in a clayey peat with wood between 100 and 77 cm depth. Whilst foraminifera were absent from the sample at 100-101 cm depth, a very low abundance assemblage comprising *J. macrescens* and *M. fusca* with some *Haplophragmoides* was recovered from the clayey peat, and the radiocarbon date at 92 cm depth indicates it was accumulating by 3660 ± 40 ^{14}C a BP.

Above 77 cm depth, the core comprises heavily iron-stained clay with some woody fragments. Foraminiferal analysis reveals a similar assemblage to that of the underlying clayey peat, and an AMS radiocarbon date of 3480 ± 50 ^{14}C a BP from 75 cm depth suggests this transition is not associated with a significant break in accumulation. Given that the core is recovered from reclaimed land, it is likely that the reduction in organic content and heavy iron-staining reflect post-depositional modification of the upper part of the sequence.

At Coonagh East (MS4), situated about 500 m south of MS5, a much thinner sequence is recovered due to the reduced depth of the pre-Holocene surface. The core terminates in a heavily consolidated silty sand with large clasts (diamict) which is abruptly overlain by a thin unit of organic-rich clay at 369 cm depth. Analysis of foraminifera from within this unit reveals abundant salt-marsh taxa similar to those

reported from MS5, although with larger numbers of *T. inflata* (Figure 7c). The base of this organic unit is radiocarbon dated to 6400 ± 50 ^{14}C a BP.

The organic-rich salt-marsh clay grades into a well-humified peat that extends from 352 – 297 cm depth, at which point, the minerogenic content increases to form half a metre of organic clay and clayey peat that finally becomes a light grey clay with some organic fragments above 254 cm depth. Foraminifera are present throughout this gradual transition and the assemblages are once again characterised by salt-marsh taxa, including a significant presence (typically >10%) of *T. inflata*. AMS radiocarbon dates from the bottom, middle and top of this interval returned ages of 5670 ± 40, 5660 ±50 and 5790 ± 40 ^{14}C a BP respectively. The slight age inversion from the uppermost date (least organic sample) may indicate incorporation of a component of allochthonous (reworked) organic matter.

The upper 250 cm of the sequence is broadly similar to the corresponding sediments in MS5, comprising light grey clay with some woody fragments which becomes increasingly iron-stained above 98 cm depth.

MS3 (near Coonagh Point) is located a little under 2 km south of MS4 but is situated adjacent to the main channel of the Shannon River. Borehole data indicates that the modern river channel is located within a broader feature cut in bedrock down to – 22 m OD (Figure 5c). The core terminates in almost 4 m of weathered diamict which is overlain by 30 cm of green-grey organic silty clay. This silty clay grades into a black, well-humified peat containing small lenses of sand. No foraminifera are present within this peat which extends from 1350 – 1182 cm depth. AMS radiocarbon dates from the bottom, lower, middle and upper portions of this peat returned ages of 9580 ± 40, 9350 ± 70, 9170 ± 40 and 8070 ± 50 ^{14}C a BP (Figure 7a).

This early Holocene basal peat includes two minerogenic units of differing character. The lower unit comprises a thin (c. 10 cm) green-grey clay with organic fragments which abruptly truncates the basal peat. Foraminiferal analysis revealed a calcareous-dominated assemblage similar in composition to the estuarine sediments recovered from lower part of MS5 (Figure 7d). Shelly material and unidentified organics from within the clay were AMS radiocarbon dated, returning ages of 7620 ± 40 and 7800 ± 40 ^{14}C a BP respectively. The upper unit consists of a thick (c. 50 cm) light grey clay

which abruptly replaces the peat beneath but grades progressively into the peat above (this gradual transition being completed by 8070 ± 50 ^{14}C a BP).

At 1182 cm depth, the humified peat unit is abruptly replaced by a thick unit of over-consolidated, occasionally laminated, grey-green clay with shells and organic fragments which extends to around 220 cm depth where it grades into a black clay. The upper 2 m of the core comprise an iron-stained silty clay with occasional organics which grades into the (modern) dark brown soil.

The final core (MS2) was recovered 3 km southeast of MS3 adjacent to Ballinacurra Creek on the southern bank of the Shannon (Figure 5b). As with MS3, the sequence terminates in diamict which is then overlain by clay and a black, well-humified peat. Disturbance of the sediments is evident within the lowermost core barrel (below 580 cm depth) and so this material is not considered further. The intact stratigraphy begins above 560 cm depth with a 1 m-thick humified silty peat with woody fragments (Figure 7a). This unit contains a very low abundance foraminiferal assemblage co-dominated by *J. macrescens* and *M. fusca*, the latter of which reaches around 40% (Figure 7e). The lower and upper parts of this silty peat are radiocarbon dated to 6500 ± 50 and 5530 ± 50 ^{14}C a BP respectively.

The silty peat grades into a laminated clayey peat which contains an abundant foraminiferal assemblage characterised by *J. macrescens*. The upper part of this unit is radiocarbon dated to 4590 ± 40 ^{14}C a BP. The sequence then continues with a woody organic clay which becomes increasingly silty and decreasingly wood-rich up core. The upper metre of the core comprises an increasingly iron-stained silty clay.

References

Ballantyne, C.K., O Cofaigh, C., 2017. The Last Irish Ice Sheet: Extent and Chronology, in: Coxon, P., McCarron, S., Mitchell, F. (Eds.), Advances in Irish Quaternary Studies. Atlantis Press, Paris, France, pp. 101–149. doi:10.29991/978-94-6239-219-9_5

Ballantyne, C.K., Wilson, P., Schnabel, C., Xu, S., 2013. Lateglacial rock slope failures in north-west Ireland: Age, causes and implications. J. Quat. Sci. 28, 789–802. doi:10.1002/jqs.2675

Brooks, A., Edwards, R., 2006. The development of a sea-level database for Ireland. Irish J. Earth Sci. 24, 13–27.

Brooks, A.J., Bradley, S.L., Edwards, R.J., Milne, G.A., Horton, B., Shennan, I., 2008. Postglacial relative sea-level observations from Ireland and their role in glacial rebound modelling. J. Quat. Sci. 23, 175–192. doi:10.1002/jqs.1119

Carter, R.W.G., 1990. The impact on Ireland of changes in mean sea-level. Programme of expert studies on climate change, Report no. 2. Department of the Environment: Dublin.

Curtis, T., Skeffington, M., 1998. The salt marshes of Ireland: an inventory and account of their geographical variation. Environ. Proc. R. Irish Acad. 98B, 87–104.

Delaney, C., Devoy, R., 1995. Evidence from sites in western Ireland of late Holocene changes in coastal environments. Mar. Geol. 124, 273–287.

Devoy, R.J.N., 1992. Questions of coastal protection and the human response to sea-level rise in Ireland and Britain. Irish Geogr. 25, 1–22.

Devoy, R.J.N., Delaney, C., Carter, R.W.G., Jennings, S.C., 1996. Coastal stratigraphies as indicators of environmental changes upon European Atlantic coasts in the late Holocene. J. Coast. Res. 12, 564–588.

de Rijk, S., 1995. Salinity control on the distribution of salt marsh foraminifera (Great Marshes, Massachusetts). J. Foraminifer. Res. 25, 156–166. doi:10.2113/gsjfr.25.2.156

Finch, T.F., 1977. Guidebook for INQUA excursion C16: Western Ireland. Geo Abstracts; Norwich. 39pp.

Healy, M.G., Hickey, K.R., 2002. Historic land reclamation in the intertidal wetlands of the Shannon estuary, western Ireland. Journal of Coastal Research 36 (special issue): 365-373.

Hickey, K.R., Healy, M.G., 2005. The reclamation of the Shannon Estuary inter-tidal flats: A case study of the Clare Slobland Reclamation Company. Irish Geography 38: 96-106.

Horton, B.P., Edwards, R.J., 2006. Quantifying Holocene Sea-Level Change Using Intertidal Foraminifera: Lessons from the British Isles, Spec. Pub. Cushman Foundation for Foraminiferal Research.

Juggins, S., 2014. C2 data analysis program ver. 1.7.7. University of Newcastle, UK.

Lambeck, K., 1996. Glaciation and sea-level change for Ireland and the Irish Sea since Late Devensian/Midlandian time. J. Geol. Soc. London 153, 853–872.

McCabe, A.M., Clark, P.U., 2003. Deglacial chronology from County Donegal, Ireland: implications for deglaciation of the British-Irish ice sheet. J. Geol. Soc. London. 160, 847–855. doi:10.1144/0016-764903-009

Orford, J.D., 1989. A review of tides, currents and waves in the Irish Sea. In The Irish Sea: A Resource at Risk. Sweeney J. (ed). Geographical Society of Ireland, Special Publication No. 3: Dublin. 18-46.

Orme, A.R., 1966. Quaternary Change of Sea-Level in Ireland. Trans. Inst. Br. Geogr. 127–140.

O'Sullivan A., 2001. Foragers, farmers and fishers in a coastal landscape: An intertidal archaeological survey of the Shannon Estuary. Royal Irish Academy: Dublin.

Pearson, G.W., 1979. Belfast radiocarbon dates IX. Radiocarbon 21: 274-90

Shaw, J., 1985. Holocene coastal evolution, Co. Donegal, Ireland. Unpublished PhD thesis. University of Ulster, Coleraine.

Shaw, J., Carter, R., 1994. Coastal peats from northwest Ireland: implications for Late Holocene RSL change and shoreline evolution. Boreas 23, 74–91.

Stephens, N., Synge, F., 1965. Late-Pleistocene shorelines and drift limits in North Donegal. Proc. R. Irish Acad. 64B, 131–153.

Wheeler, A.J., Healy, M.G. 2001. Coastal landscapes and environmental change in the Shannon estuary. In O'Sullivan A. (ed.) Foragers, farmers and fishers in a coastal landscape: An intertidal archaeological survey of the Shannon Estuary. Royal Irish Academy: Dublin.

Williams, D.M., Doyle, E., 2014. Dates from drowned Mid-Holocene landscapes on the Central Western Irish Seaboard. Irish J. Earth Sci. 32, 23–27.

Supplementary Figures

FIGURE S1: Sample elevation predicted by the foraminiferal transfer function for tide level (squares) plotted with actual elevation of surface samples (diamonds) collected from nine locations within the Shannon estuary (See Figure 5A inset). Colour coding

indicates the extent to which the surface samples have a good modern analogue in the training set.

Site	MLWST	MLWNT	MTL	MHWNT	MHWST	HAT
Ballymichael	-2.41	-1.41	-0.66	0.09	1.09	1.82
Rossadilisk	-2.41	-1.31	-0.59	0.19	1.19	2.00
L. Fhada	-2.31	-1.01	-0.16	0.79	1.89	2.55
Coonagh	-2.67	-1.87	0.14	1.52	2.94	3.39

Table S1: Summary tidal characteristics of the study areas (m OD Malin) based on Admiralty Tide Tables. MLWST = Mean low water spring tide; MLWNT = Mean low water neap tide; MTL = Mean tide level MHWNT = Mean high water neap tide; MHWST = Mean high water spring tide; HAT = Highest astronomical tide.

						Radiocarbon Age (^{14}C a BP)		Calibrated Age (Cal. a BP)	
Site	Manuscript Code	Lab Code	Material	δ^{13}C (‰)	Depth (cm)	Age	Error	Min	Max
Ballymichael	-	Beta-216639	Peat	-	295	11430	40	13155	13375
Rossadilisk	-	Beta-211391	Peat	-22.5	519	12250	40	14004	14237
L Fhada	-	SUERC-33216	Peat	-20.9	868	10280	40	11828	12375
L Fhada	-	SUERC-33217	Peat	-25.2	892	11150	40	12876	13106
L Fhada	-	SUERC-33218	Peat	-20.8	985	11860	50	13567	13766
Meelick (MS5)	1	BETA 211398	Org Sed	-27.8	75	3480	50	3618	3880
Meelick (MS5)	2	BETA 203549	Peat	-27.5	94	3660	40	3874	4138
Meelick (MS5)	3	BETA 203547	Peat	-26.3	214	4030	40	4417	4783
Meelick (MS5)	4	BETA 203548	Peat	-25.5	293	5860	40	6562	6778
Coonagh East (MS4)	5	BETA 211397	Org Sed	-24.8	254	5790	40	6485	6711
Coonagh East (MS4)	6	BETA 203544	Peat	-25.2	276	5660	50	6311	6562
Coonagh East (MS4)	7	BETA 203546	Org Sed	-25.6	295	5670	40	6322	6558
Coonagh East (MS4)	8	BETA 203545	Org Sed	-25.7	366	6400	50	7256	7424
Ballinacurra (MS2)	9	BETA 203540	Peat	-25.5	363	4590	40	5057	5459
Ballinacurra (MS2)	10	BETA 203539	Peat	-26.7	47	5530	50	6215	6412
Ballinacurra (MS2)	11	BETA 203538	Peat	-27.6	55	6500	50	7306	7551
Coonagh Pt. (MS3)	12	BETA 203537	Peat	-27.5	1224	8070	50	8770	9128
Coonagh Pt. (MS3)	13	BETA 203541	Peat	-28.1	1292	9170	40	10237	10482
Coonagh Pt. (MS3)	14	BETA 203542	Peat	-28.8	1308	9350	70	10298	10741
Coonagh Pt. (MS3)	15	BETA 203543	Peat	-27.6	1348	9580	40	10741	11121

Meelick (MS5)	16	BETA 211399	Shell	-5.8	1331	7120	50	7493	7770
Meelick (MS5)	16	BETA 216647	Foram	-14.4	1331	7390	70	7682	8049
Coonagh Pt. (MS3)	17	BETA 211395	Org Sed	-27.2	1335	7800	40	8454	8645
Coonagh Pt. (MS3)	17	BETA 211396	Shell	-10.3	1335	7620	40	7973	8269

Table S2: New radiocarbon dates from the study sites. Manuscript codes refer to the Shannon sea-level data.

Supplementary File

Edwardsetal_SuppInfo.xlsx

Excel datasheet of microfossil counts (diatoms, foraminifera and pollen) for the fossil material referred to in the text.

FIGURE 1

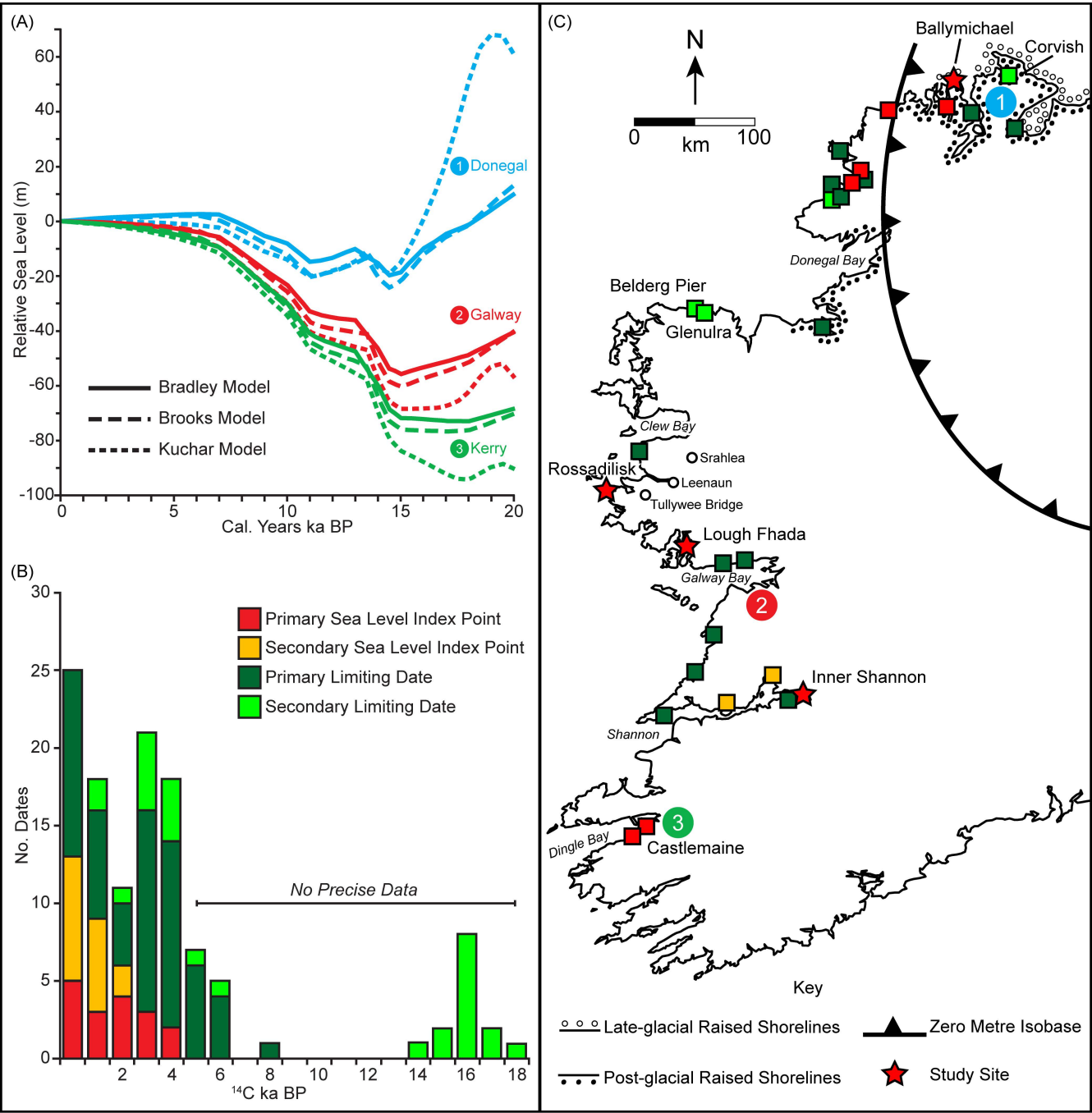
(A)
Relative Sea Level (m)
Cal. Years ka BP
1 Donegal
2 Galway
3 Kerry
Bradley Model
Brooks Model
Kuchar Model
(B)
No. Dates
^{14}C ka BP
Primary Sea Level Index Point
Secondary Sea Level Index Point
Primary Limiting Date
Secondary Limiting Date
No Precise Data
(C)
N
0
km
100
Ballymichael
Corvish
Donegal Bay
Belderg Pier
Glenulra
Clew Bay
Rossadilisk
Srahlea
Leenaun
Tullywee Bridge
Lough Fhada
Galway Bay
Inner Shannon
Shannon
Dingle Bay
Castlemaine
Key
Late-glacial Raised Shorelines
Post-glacial Raised Shorelines
Zero Metre Isobase
Study Site

Figure 2

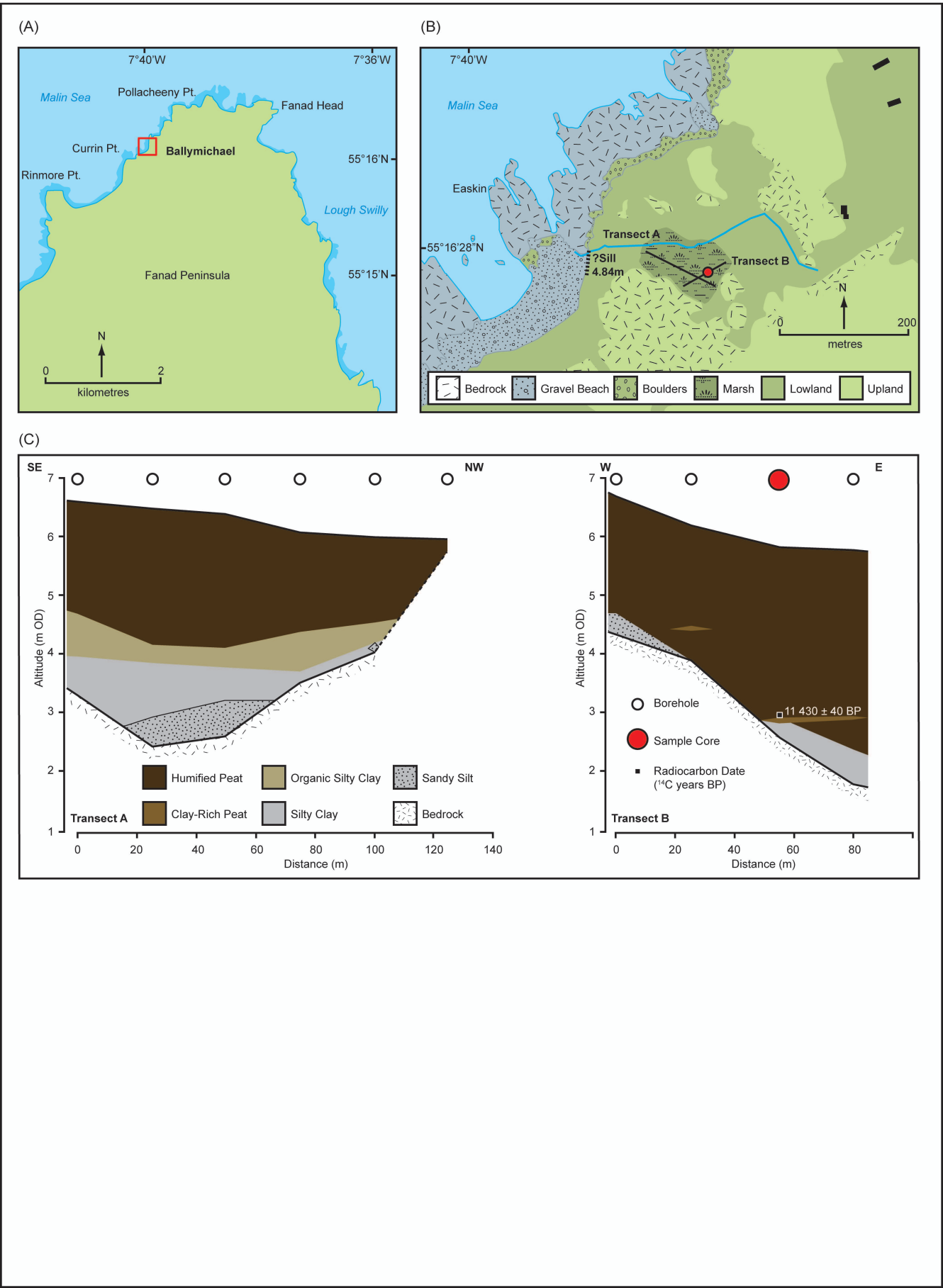
(A)
7°40'W
7°36'W
Malin Sea
Pollacheeny Pt.
Fanad Head
Currin Pt.
Ballymichael
55°16'N
Rinmore Pt.
Lough Swilly
Fanad Peninsula
55°15'N
N
0
2
kilometres
(B)
7°40'W
Malin Sea
Easkin
55°16'28"N
Transect A
?Sill
4.84m
Transect B
N
0
200
metres
Bedrock
Gravel Beach
Boulders
Marsh
Lowland
Upland
(C)
SE
NW
Altitude (m OD)
Humified Peat
Organic Silty Clay
Sandy Silt
Transect A
Clay-Rich Peat
Silty Clay
Bedrock
Distance (m)
W
E
Borehole
11 430 ± 40 BP
Sample Core
Radiocarbon Date
(14C years BP)
Transect B
Distance (m)

Figure 3

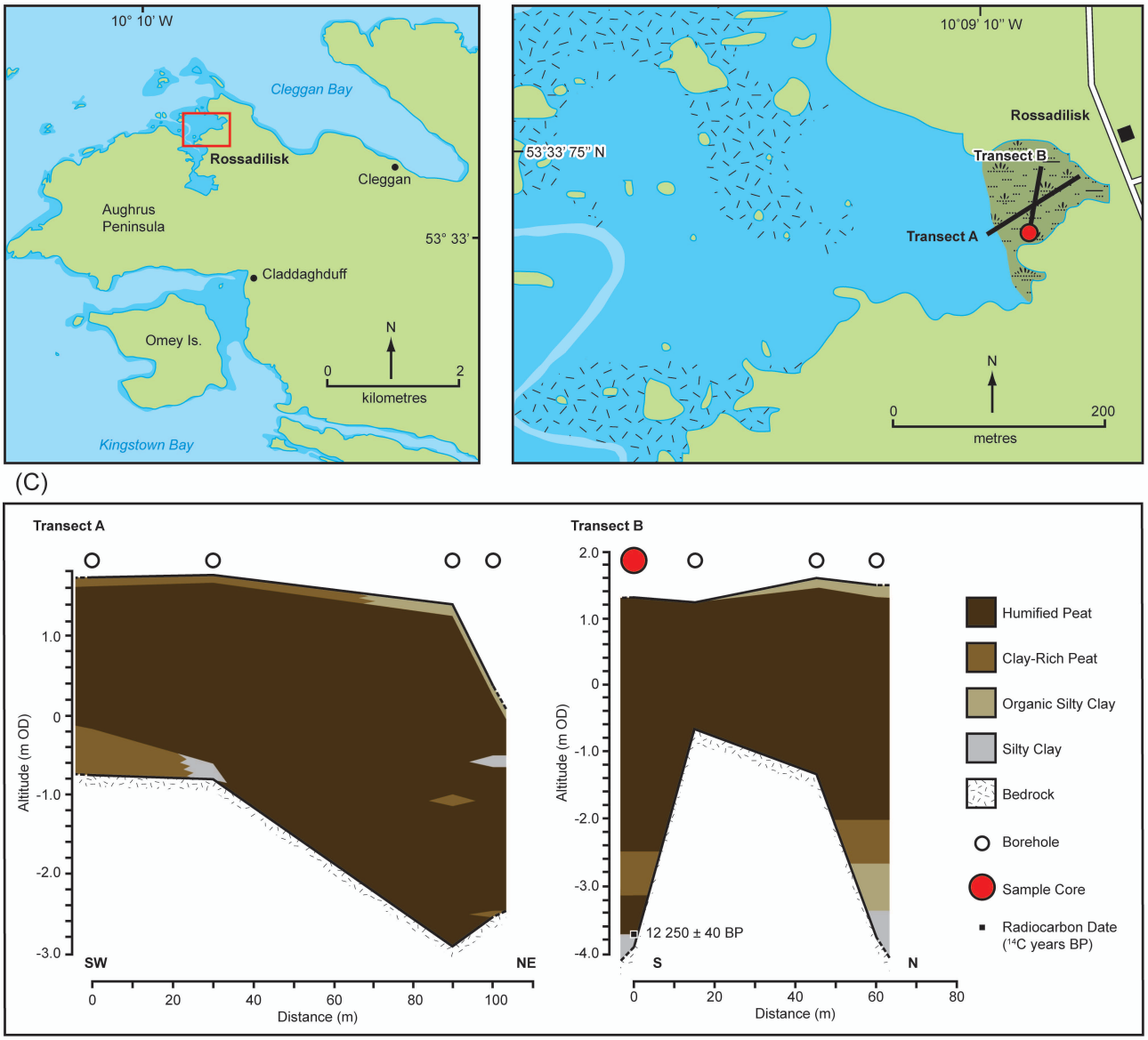
(A)
10° 10' W
Cleggan Bay
Rossadilisk
Cleggan
Aughrus
Peninsula
53° 33'
Claddaghduff
Omey Is.
N
0
2
kilometres
Kingstown Bay
(B)
10°09' 10" W
53°33' 75" N
Rossadilisk
Transect B
Transect A
N
0
200
metres
(C)
Transect A
Transect B
Altitude (m OD)
1.0
0
-1.0
-2.0
-3.0
SW
NE
0
20
40
60
80
100
Distance (m)
2.0
-4.0
12 250 ± 40 BP
S
N
Humified Peat
Clay-Rich Peat
Organic Silty Clay
Silty Clay
Bedrock
Borehole
Sample Core
Radiocarbon Date
(14C years BP)

Figure 4

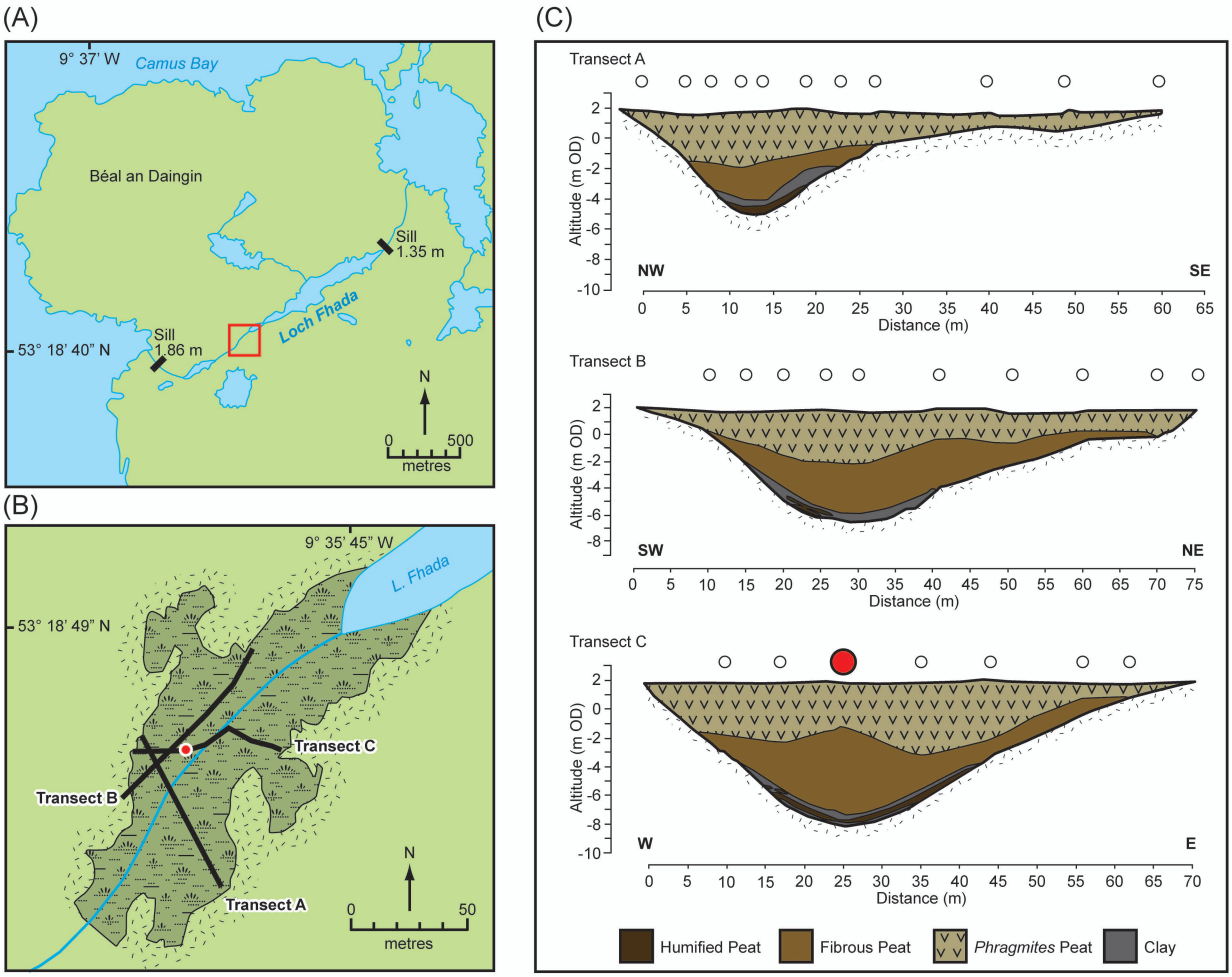
(A)
9° 37' W
Camus Bay
Béal an Daingin
Sill
1.35 m
Loch Fhada
Sill
1.86 m
53° 18' 40" N
N
0
500
metres
(B)
9° 35' 45" W
L. Fhada
53° 18' 49" N
Transect C
Transect B
Transect A
N
0
50
metres
(C)
Transect A
Altitude (m OD)
NW
SE
Distance (m)
Transect B
SW
NE
Distance (m)
Transect C
W
E
Distance (m)
Humified Peat
Fibrous Peat
Phragmites Peat
Clay

Figure 5

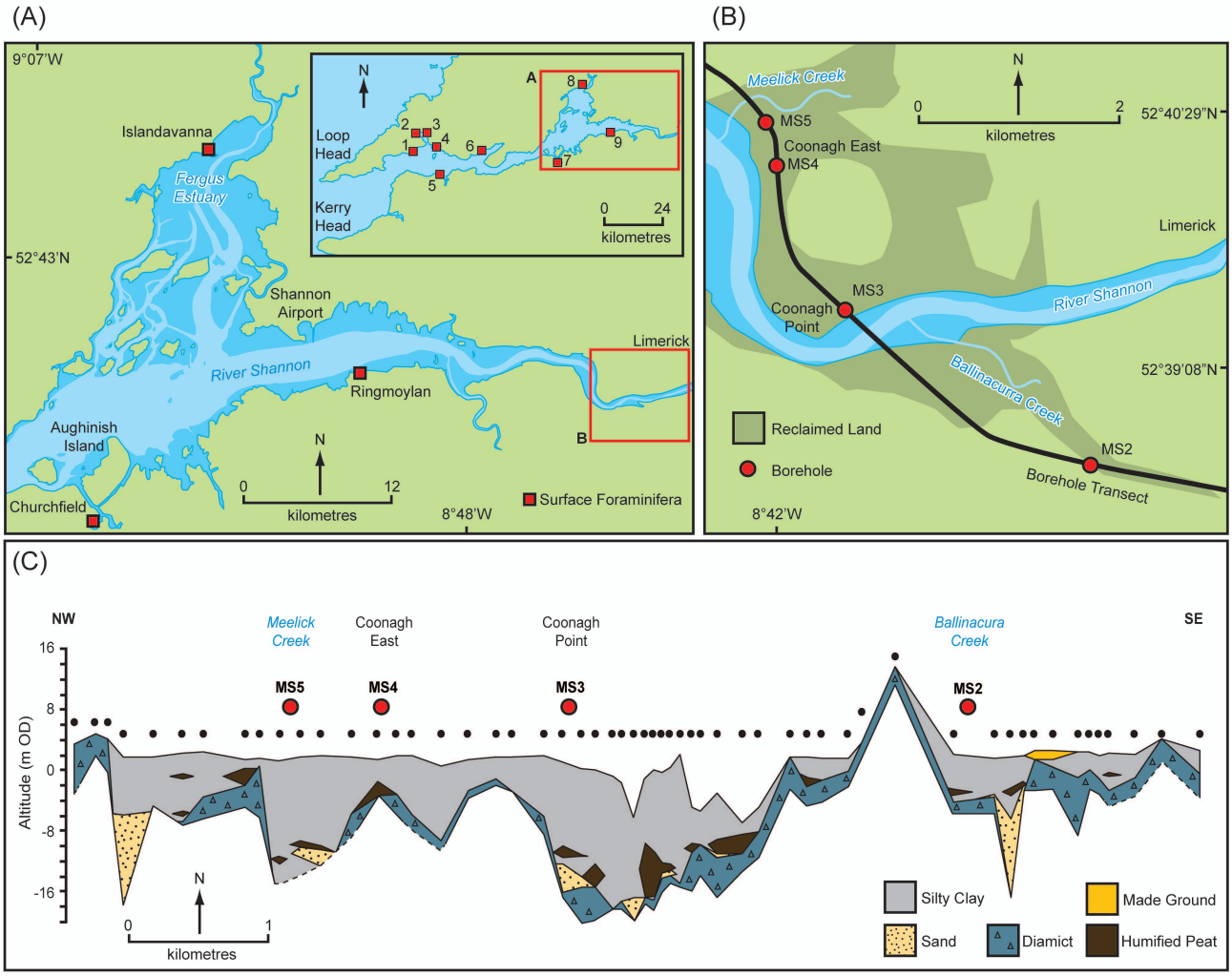
(A)
9°07'W
52°43'N
8°48'W
Islandavanna
Fergus Estuary
Loop Head
Kerry Head
A
B
Shannon Airport
River Shannon
Ringmoylan
Limerick
Aughinish Island
Churchfield
N
0 12
kilometres
0 24
kilometres
Surface Foraminifera
(B)
Meelick Creek
MS5
Coonagh East
MS4
MS3
Coonagh Point
River Shannon
Limerick
Ballinacurra Creek
MS2
Borehole Transect
52°40'29"N
52°39'08"N
8°42'W
0 2
kilometres
Reclaimed Land
Borehole
(C)
NW
SE
Meelick Creek
Coonagh East
Coonagh Point
Ballinacurra Creek
MS5
MS4
MS3
MS2
Altitude (m OD)
16
8
0
-8
-16
0 1
kilometres
Silty Clay
Made Ground
Sand
Diamict
Humified Peat

Figure 6

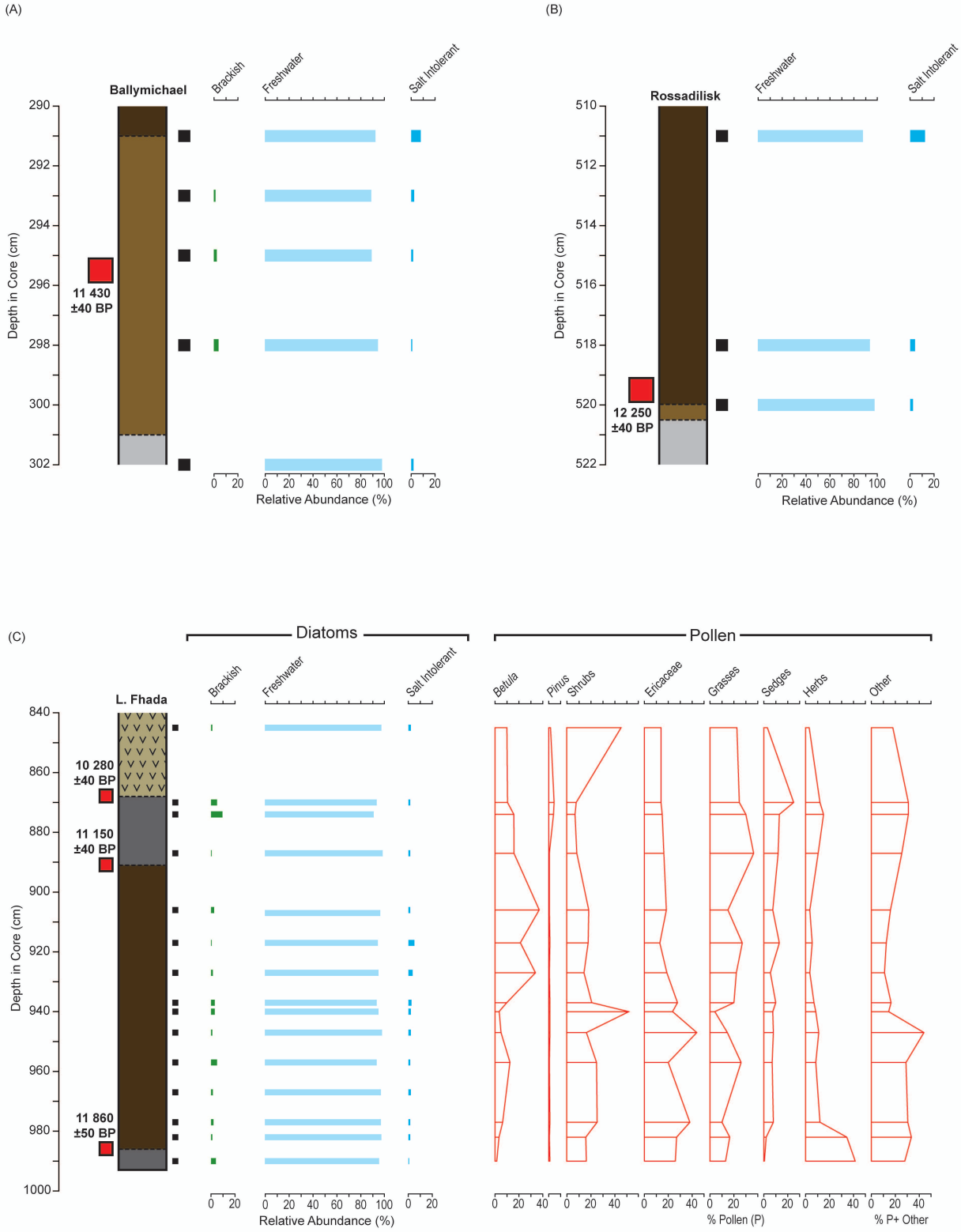
(A)
Ballymichael
Brackish
Freshwater
Salt Intolerant
Depth in Core (cm)
290
292
294
296
298
300
302
11 430
±40 BP
0 20
0 20 40 60 80 100
0 20
Relative Abundance (%)
(B)
Rossadilisk
Freshwater
Salt Intolerant
Depth in Core (cm)
510
512
514
516
518
520
522
12 250
±40 BP
0 20 40 60 80 100
0 20
Relative Abundance (%)
(C)
Diatoms
Pollen
L. Fhada
Brackish
Freshwater
Salt Intolerant
Betula
Pinus
Shrubs
Ericaceae
Grasses
Sedges
Herbs
Other
Depth in Core (cm)
840
860
880
900
920
940
960
980
1000
10 280
±40 BP
11 150
±40 BP
11 860
±50 BP
0 20
0 20 40 60 80 100
0 20
Relative Abundance (%)
0 20 40
0 20 40
0 20 40
0 20
0 20
0 20 40
0 20 40
% Pollen (P)
% P+ Other

Figure 7

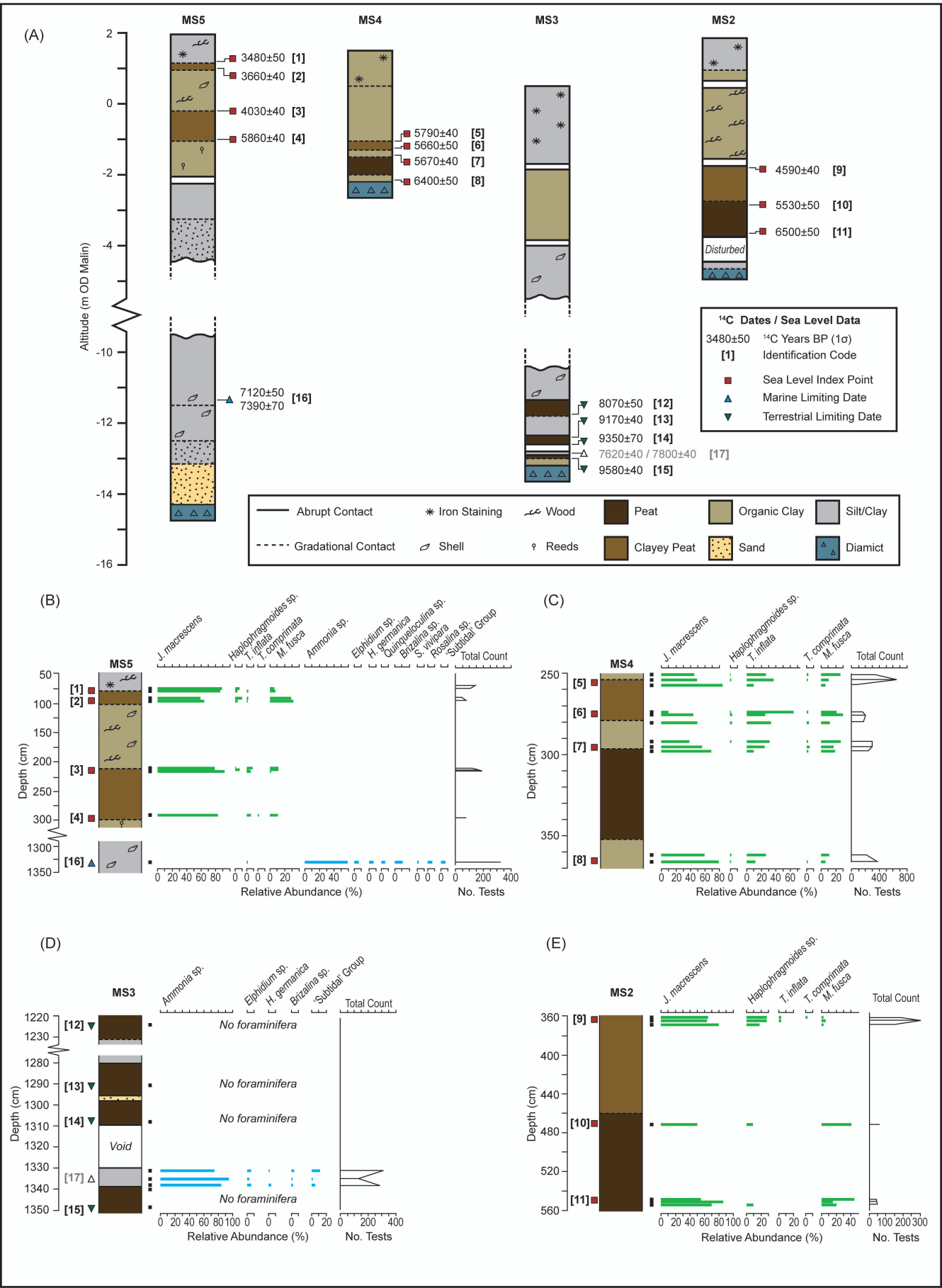
(A)
MS5
MS4
MS3
MS2
Altitude (m OD Malin)
3480±50 [1]
3660±40 [2]
4030±40 [3]
5860±40 [4]
5790±40 [5]
5660±50 [6]
5670±40 [7]
6400±50 [8]
4590±40 [9]
5530±50 [10]
6500±50 [11]
Disturbed
7120±50
7390±70 [16]
8070±50 [12]
9170±40 [13]
9350±70 [14]
7620±40 / 7800±40 [17]
9580±40 [15]
14C Dates / Sea Level Data
3480±50 14C Years BP (1σ)
[1] Identification Code
Sea Level Index Point
Marine Limiting Date
Terrestrial Limiting Date
Abrupt Contact
Gradational Contact
Iron Staining
Shell
Wood
Reeds
Peat
Clayey Peat
Organic Clay
Sand
Silt/Clay
Diamict
(B)
MS5
J. macrescens
Haplophragmoides sp.
T. inflata
T. comprimata
M. fusca
Ammonia sp.
Elphidium sp.
H. germanica
Quinqueloculina sp.
Brizalina sp.
S. vulpara
Rosalina sp.
'Subtidal' Group
Total Count
Depth (cm)
Relative Abundance (%)
No. Tests
(C)
MS4
(D)
MS3
No foraminifera
Void
(E)
MS2

Figure 8

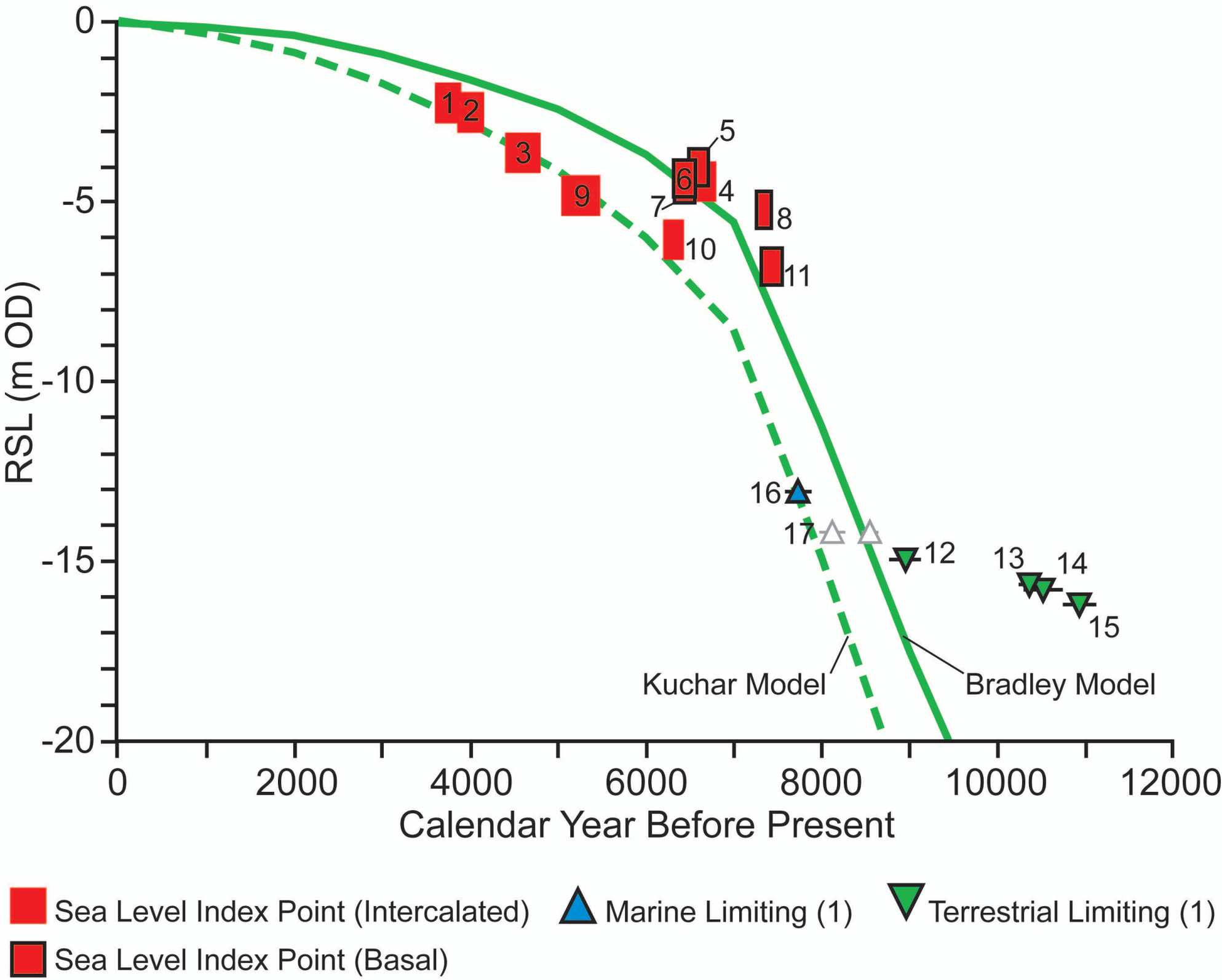
0
-5
-10
-15
-20
RSL (m OD)
0
2000
4000
6000
8000
10000
12000
Calendar Year Before Present
1
2
3
9
5
6
4
7
8
10
11
16
17
12
13
14
15
Kuchar Model
Bradley Model
Sea Level Index Point (Intercalated)
Marine Limiting (1)
Terrestrial Limiting (1)
Sea Level Index Point (Basal)

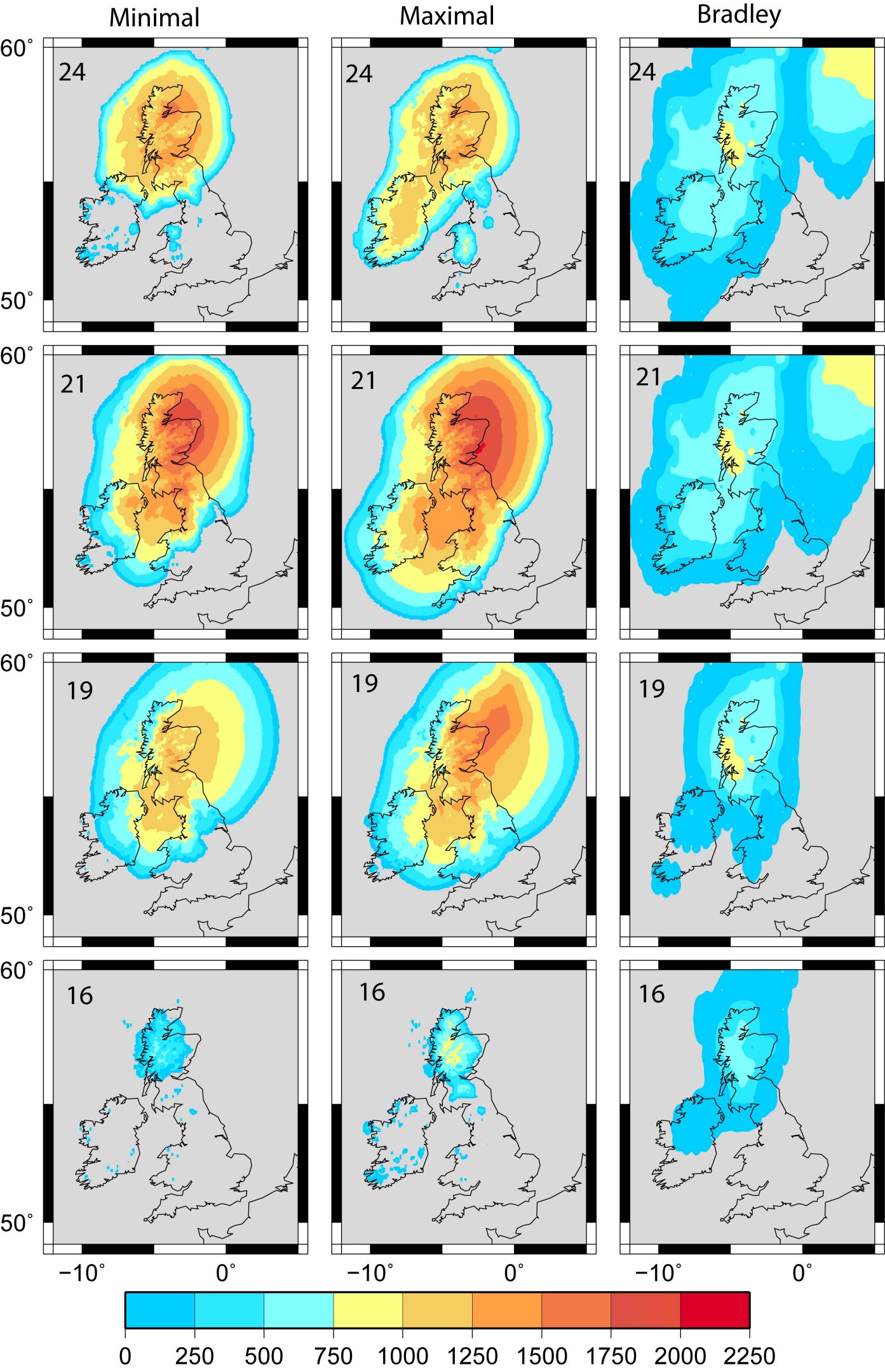
Minimal
Maximal
Bradley
24
21
19
16
60°
50°
−10°
0°
0
250
500
750
1000
1250
1500
1750
2000
2250

Figure 10

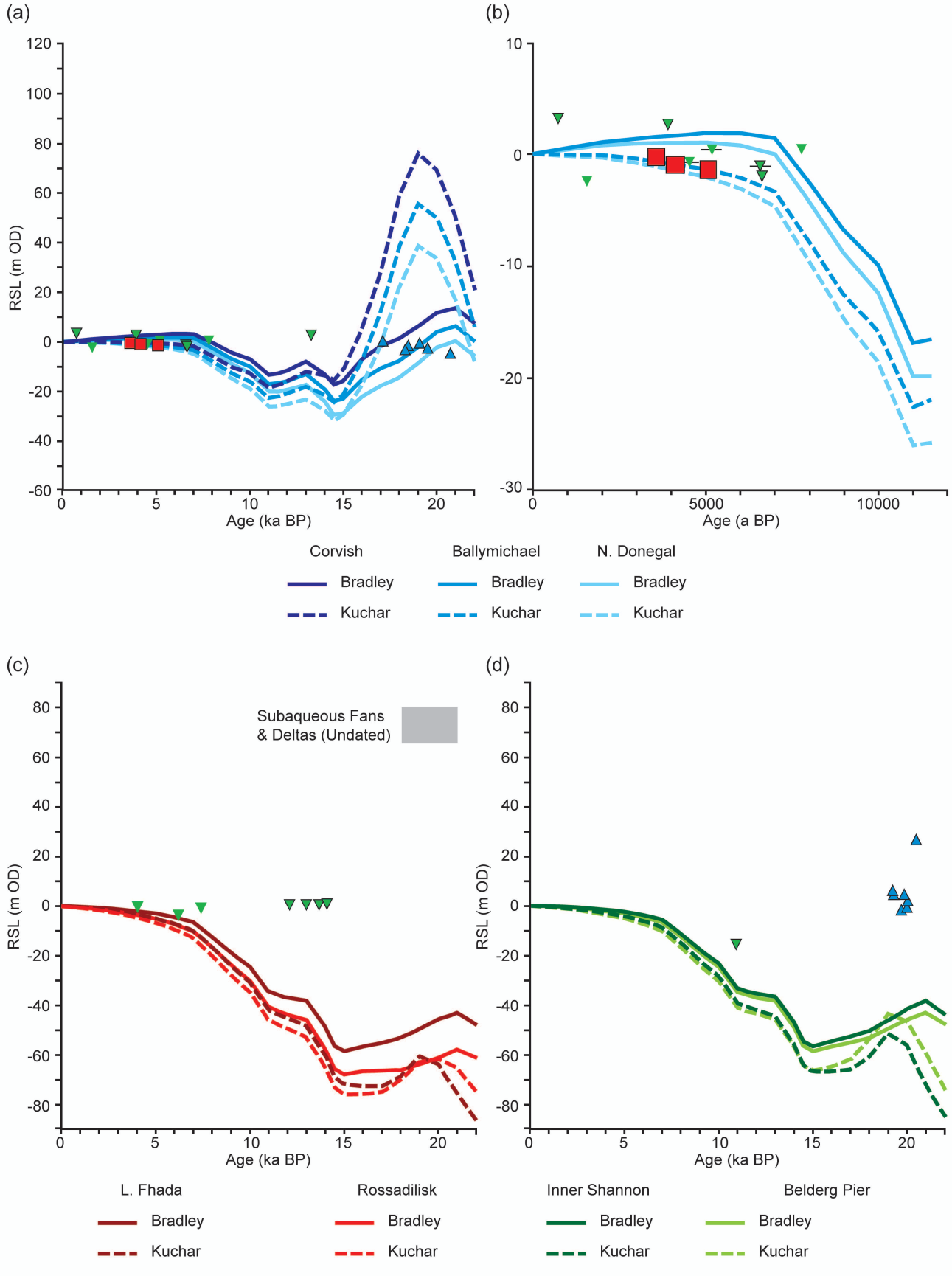
(a)
(b)
RSL (m OD)
Age (ka BP)
Age (a BP)
Corvish
Ballymichael
N. Donegal
Bradley
Kuchar
(c)
(d)
Subaqueous Fans
& Deltas (Undated)
L. Fhada
Rossadilisk
Inner Shannon
Belderg Pier

Figure 11

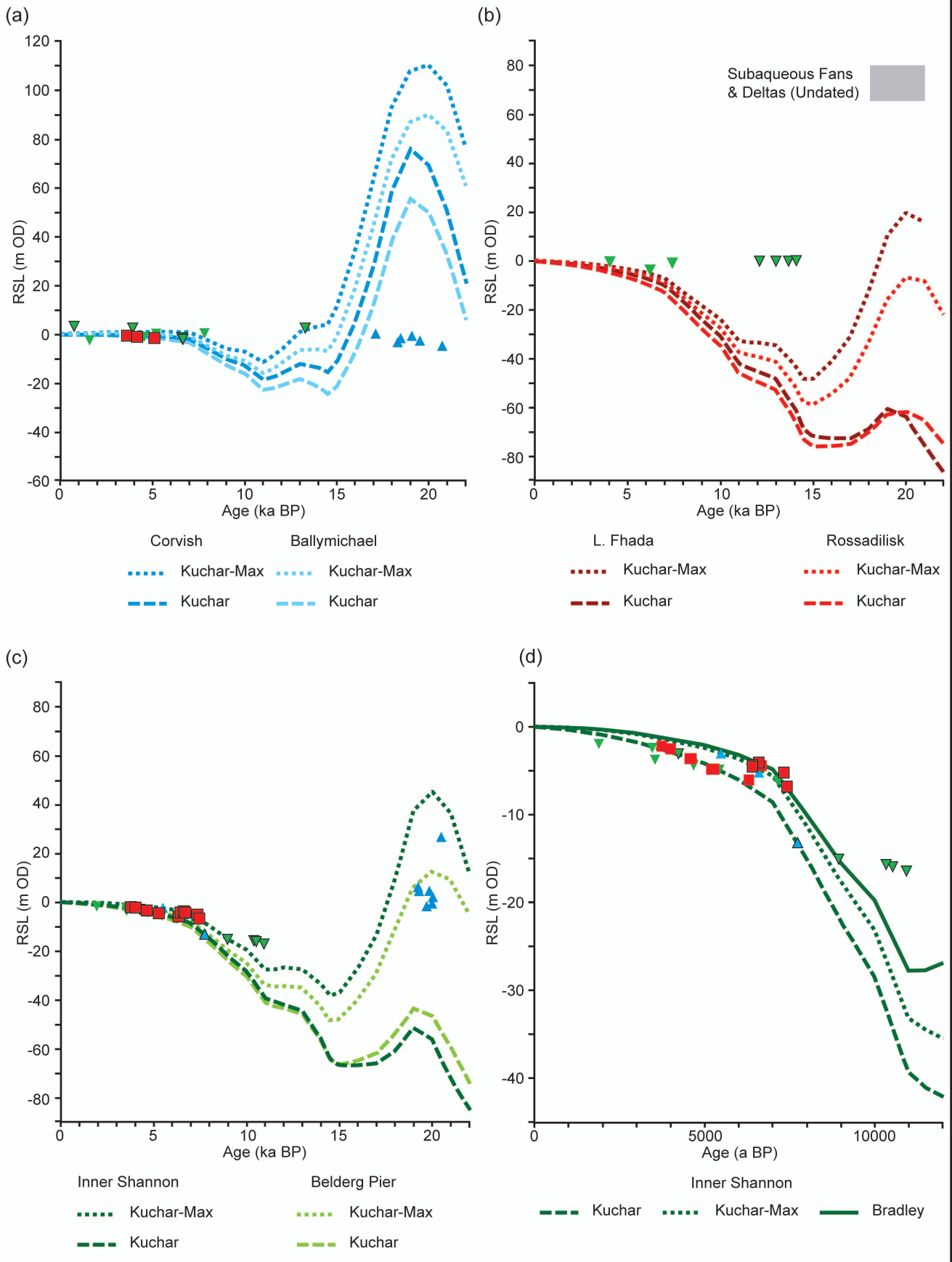
(a)
RSL (m OD)
Age (ka BP)
Corvish
Kuchar-Max
Kuchar
Ballymichael
Kuchar-Max
Kuchar
(b)
Subaqueous Fans
& Deltas (Undated)
RSL (m OD)
Age (ka BP)
L. Fhada
Kuchar-Max
Kuchar
Rossadilisk
Kuchar-Max
Kuchar
(c)
RSL (m OD)
Age (ka BP)
Inner Shannon
Kuchar-Max
Kuchar
Belderg Pier
Kuchar-Max
Kuchar
(d)
RSL (m OD)
Age (a BP)
Inner Shannon
Kuchar
Kuchar-Max
Bradley

Figure S1

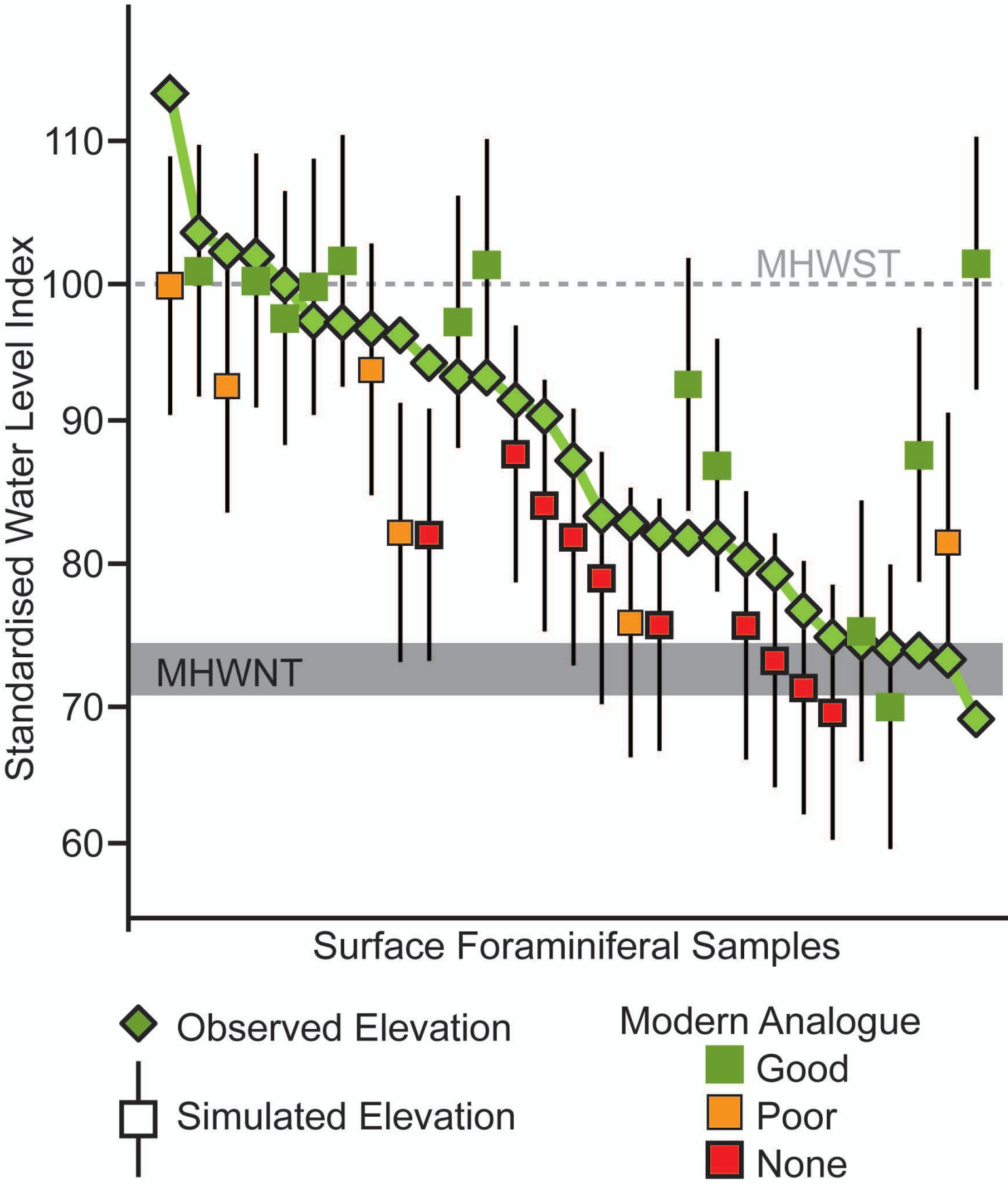
110
100
90
80
70
60
Standardised Water Level Index
MHWST
MHWNT
Surface Foraminiferal Samples
Observed Elevation
Simulated Elevation
Modern Analogue
Good
Poor
None